Title

Induction of core symptoms of autism spectrum disorders by in vivo CRISPR/Cas9-based gene editing in the brain of adolescent rhesus monkeys

Authors

Shi-Hao Wu[1, 2, 4, †], Xiao Li[1,10, †], Dong-Dong Qin[9, †], Lin-Heng Zhang[2, 5, †], Tian-Lin Cheng[1], Zhi-Fang Chen[1], Bin-Bin Nie[6, 7], Xiao-Feng Ren[2, 5], Jing Wu[2], Wen-Chao Wang[2], Ying-Zhou Hu[2], Yilin Gu[2], Long-Bao Lv[4], Yong Yin[8, *], Xin-Tian Hu[2, 3, 4,*], Zi-Long Qiu[1, 3, 11, *]

Affiliations

[1] Institute of Neuroscience, State Key Laboratory of Neuroscience, CAS Key Laboratory of Primate Neurobiology, Chinese Academy of Sciences, Shanghai, 200031, China.

[2] Kunming Institute of Zoology, Chinese Academy of Sciences, Kunming, Yunnan, 650223, China.

[3] Center for Excellence in Brain Science and Intelligence Technology, Chinese Academy of Sciences, Shanghai, 200031, China.

[4] Kunming Primate Research Center, Kunming Institute of Zoology, Chinese Academy of Sciences, Kunming, Yunnan, 650223, China.

[5] Kunming College of Life Science, University of the Chinese Academy of Sciences, Kunming, Yunnan, 650204, China.

[6] Beijing Engineering Research Center of Radiographic Techniques and Equipment, Institute of High Energy Physics, Chinese Academy of Sciences, Beijing 100049, China.

[7] School of Nuclear Science and Technology, University of Chinese Academy of Sciences, Beijing 100049, China.

[8] Department of Rehabilitation Medicine, Fourth Affiliated Hospital of Kunming Medical University, Kunming, Yunnan, 650021, China.

[9] Yunnan University of Traditional Chinese Medicine, 1076 Yuhua Road, Kunming, Yunnan, 650500, China.

28   [10] Academy for Engineering & Technology, Fudan University, Shanghai, 200433, China.

29   [11] Lead Contact.

30   †These authors contributed equally to this work.

31   *Co-corresponding authors (zqiu@ion.ac.cn, xthu@mail.kiz.ac.cn).

32   **Keywords:** Autism spectrum disorders; Nonhuman primate model; disease model; Gene-editing;

33

34   **Abstract**

35   Although CRISPR/Cas9-mediated gene editing is widely applied to mimic human disorders,

36   whether acute manipulation of disease-causing genes in the brain leads to behavioral abnormalities

37   in non-human primates remains to be determined. Here we induced genetic mutations in MECP2,

38   a critical gene linked to Rett syndrome (RTT) and autism spectrum disorders (ASDs), in the

39   hippocampus (DG and CA1–4) of adolescent rhesus monkeys (Macaca mulatta) in vivo via adeno-

40   associated virus (AAV)-delivered Staphylococcus aureus Cas9 with sgRNAs targeting MECP2.

41   In comparison to monkeys injected with AAV-SaCas9 alone (n = 4), numerous autistic-like

42   behavioral abnormalities were identified in the AAV-SaCas9-sgMECP2-injected monkeys (n = 7),

43   including social interaction deficits, abnormal sleep patterns, insensitivity to aversive stimuli,

44   abnormal hand motions and defective social reward behaviors. Furthermore, some aspects of

45   ASDs and RTT, such as stereotypic behaviors, did not appear in the MECP2 gene-edited monkeys,

46   suggesting that different brain areas likely contribute to distinct ASD symptoms. This study

47   showed that acute manipulation of disease-causing genes via in vivo gene editing directly led to

48   behavioral changes in adolescent primates, paving the way for the rapid generation of genetically

49   engineered non-human primate models for neurobiological studies and therapeutic development.

50

51

Introduction

Discovery of the clustered regularly interspaced short palindromic repeats (CRISPR)-associated protein (Cas9) system in bacteria and its optimization of genome editing have permitted efficient site-specific genetic manipulation in various mammalian cells and postmitotic tissues [1-4].

Gene editing has been successfully used in germline cells to create genetically engineered animals, including non-human primates, in order to mimic human brain disorders [5-9]. Since 2014, researchers have established genetically engineered non-human primates with CRISPR/Cas9 technology [10-12]. Moreover, various studies have identified the possibility of using CRISPR/Cas9 to generate non-human primate models for human disease [13-16].

In particular, adeno-associated virus (AAV)-delivered Staphylococcus aureus Cas9 (SaCas9) or Streptococcus pyogenes Cas9 (SpCas9) approaches can be applied to edit liver and muscle tissue genes in vivo with high efficiency [17-20], and viral vector-based gene editing is widely used in primate nervous system disease research, especially Parkinson's disease [21-23]. However, it remains unknown whether direct in vivo gene editing in the adult brain of non-human primates can lead to ASD-related phenotypes, which would facilitate the modeling process and avoid the prolonged reproduction period required for primate species.

Genetic manipulation of MECP2, a critical gene in Rett syndrome (RTT) and autism spectrum disorders (ASDs), by lentiviral-based transgenic methods or transcription activator-like effector nuclease (TALEN)-based gene editing in non-human primates can result in autistic-like symptoms and faithfully mimic many aspects of MECP2-related disorders [9, 24-26]. However, their long reproduction cycles and inconvenience of international transfer have prevented the wide application of non-human primates as disease models. Thus, we investigated whether acute manipulation of the MECP2 gene via viral-delivered gene editing in adolescent rhesus macaque brains can lead to autism-related behavioral abnormalities, which should help facilitate disease modeling in non-human primates and address the role of MECP2 in particular brain regions, as well as assist in vivo neural circuitry research in non-human primates.

81

Results

Design of AAV-SaCas9 and sgRNA vectors and validation of efficiency of *in vivo* gene editing

Taking advantage of the small-sized Cas9 protein — *Staphylococcus aureus* Cas9 (SaCas9), we used AAV-mediated SaCas9 to delete the *MECP2* gene in the rhesus macaque brains *in vivo* and determine whether this leads to behavioral abnormalities [4]. To target the *MECP2* gene in the monkey genome, we synthesized two sgRNAs specifically targeting exon 4 in *MECP2* (Fig. 1A, B). The two sgRNAs (sgRNA-MECP2-a, b) were individually inserted into the AAV-hSyn-SaCas9-U6-sgRNA vector, with each harboring the human synapsin promoter to drive SaCas9 and U6 promoter to drive the sgRNA cassette. We used the AAV-hSyn-SaCas9-U6-sgRNA vector with sgRNA targeting the LacZ enzyme as the control vector.

92

To ensure complete deletion of *MECP2*, we injected two AAV-hSyn-SaCas9-U6-sgMECP2-a/b vectors and AAV-hSyn-GFP (green fluorescent protein indicating injection site) into the Cas9-MECP2 monkey group (n = 7, age: 2–3 years). We injected AAV-hSyn-SaCas9-U6-sgLacZ and AAV-hSyn-GFP into the Cas9-Control monkey group (n = 4, age: 2–3 years) (Table S1A-I).

97

The hippocampus is recognized as a critical region for social memory [27, 28]. Thus, we examined whether deletion of *MECP2* in the monkey hippocampus leads to autistic-like phenotypes. To localize the hippocampus precisely in the monkey brain, a magnetic resonance imaging (MRI)-based deep brain structure localization procedure (with an error < 1.0 mm) was applied (Fig. S1). After localization, we injected the AAVs into ~40 sites on each side of the hippocampus (Fig. 1C, D, see Table S2 for injection coordinates and injected virus volumes, and figure legends and Methods for technical details) [29, 30].

105

To confirm the efficiency of gene editing, we amplified the sgRNA-targeting genomic regions from monkey hippocampal tissues via polymerase chain reaction (PCR). We identified critical genetic mutations in these regions, including stop-codons, thus showing the effectiveness of SaCas9-mediated gene editing (Fig. S2). To further determine whether the MECP2 protein level was altered by gene editing, we performed immunohistochemical experiments on sections of the monkey hippocampus. Results showed that the MECP2 protein level decreased significantly in the

112 hippocampus of the Cas9-MECP2 monkeys compared with that of the Cas9-Control monkeys (Fig.

113 1E-F). This indicated that the CRISPR/Cas9 system effectively reduced the expression of

114 endogenous MECP2 in the monkey brain via gene editing. To rule out the possibility of SaCas9-

115 mediated off-target genome editing, we identified potential genomic off-target sites in the

116 hippocampal tissue of injected monkeys. However, the top three off-target site candidates of each

117 sgRNA showed no signs of off-site genome editing in protein-coding regions (Fig. S3).

118

119 To determine whether viral injections in the monkey brain cause unexpected neuroinflammation

120 effects and inflammation-mediated destruction of transduced cells, immunohistochemical

121 experiments were performed on the monkey hippocampal slides. We found that both astrocyte and

122 microglial cells exhibited negative activation signals, e.g., numbers of GFAP- and Iba1-positive

123 cells as well as process lengths and endpoints of Iba1-positive cells (Fig. S4A-F).

124

125 **Examination of social behaviors within a community**

126 According to the Diagnostic and Statistical Manual of Mental Disorders (5th Edition, DSM-V)

127 and clinical diagnostic criteria for RTT and ASDs [31-33], we designed several behavioral assays

128 to analyze the core behavioral phenotypes of monkeys after viral injection for 3–6 months (Table

129 S1A). We first compared the behavioral phenotypes for individual monkeys before and after viral

130 injection. As the rhesus monkeys were not inbred strains, comparison of behaviors with or without

131 manipulation of individual monkeys can serve as a reliable parameter. We also examined the role

132 of *MECP2* in these behaviors by comparing the gene-edited group (Cas9-MECP2) with the control

133 group (Cas9-Control). Abnormality in social interactions and communication are hallmarks of

134 ASDs. To observe the natural behaviors of monkeys within a social community, we established

135 several social groups (each consisting of 6–8 age-matched male monkeys, including one or two

136 gene-edited monkeys). All behaviors were video-recorded and then analyzed off-line to examine

137 the various behaviors of individual monkeys before and after gene editing, as well as between the

138 Cas9-MECP2 and Cas9-Control groups [9].

139

140 Firstly, the duration of active social contact, defined as initiating play, sharing toys, grooming

141 others, and sitting together [9], was significantly decreased after the Cas9-MECP2 virus injection

142 (monkey number, n = 7) compared to baseline prior to viral injection (Movie S1, S2, S3), but was

143   not observed in the Cas9-Control group (monkey number, n = 3) (Fig. 2A-C). After gene editing,

144   the Cas9-MECP2 group also exhibited significantly less active social contact compared with the

145   Cas9-Control group (Fig. 2D). The frequency of active social contact was not altered with injection

146   of either Cas9-MECP2 or Cas9-Control virus (Fig. 2E, F). The frequency of active social contact

147   in the Cas9-MECP2 group displayed a decreasing (but non-significant) trend compared with the

148   Cas9-Control group (Fig. 2G, H). The significant difference in social interaction before and after

149   injection of the Cas9-MECP2 virus suggests that *MECP2* in the hippocampus plays a critical role

150   in regulating social interaction in monkeys.

151

152   **Altered aggressive-like behaviors in monkeys following *MECP2* gene editing**

153   It is well documented that ASD individuals in human communities are often at a higher risk of

154   being bullied [34]. We reasoned that, due to altered social behaviors, the *MECP2* gene-edited

155   monkeys may hold inferior social positions and, as a result, display less aggressive behaviors. Thus,

156   we determined whether aggressive and submissive behaviors were altered in gene-edited monkeys

157   in the social community described above. We found that active attack behaviors, such as biting,

158   slapping, grabbing, and stare threatening, were significantly decreased in monkeys injected with

159   the Cas9-MECP2 virus, which was not found in the Cas9-Control group (Fig. 3A, B, C). The Cas9-

160   MECP2 group exhibited significantly less active aggressive behaviors compared with the Cas9-

161   Control group after viral injection (Fig. 3D).

162

163   Consequently, submissive behaviors, such as screaming threat, crouching, fleeing, lip smacking,

164   grimacing, submissive presenting, or escaping, increased remarkably after injection of the Cas9-

165   MECP2 virus compared to injection of the Cas9-Control virus (Fig. 3E, F, G, H). This evidence

166   indicates that Cas9-MECP2-mediated gene editing significantly altered social interactions,

167   strongly suggesting that manipulation of the *MECP2* gene is sufficient to modulate social

168   behaviors in adolescent monkeys.

169

170   **Abnormal circadian activity and sleep patterns in monkeys following *MECP2* manipulations**

171   Sleep problems are a prominent feature of ASDs and RTT [32, 35-37]. To address whether sleep

172   patterns can be altered by *in vivo MECP2* gene editing, we used collar-like monitors (Actical

173   physical activity monitors, Respironics, Pennsylvania, USA) belt-fixed onto the necks of the

174   monkeys for 7–9 d (according to the battery life) to record 24-h activity (Table S1B). After off-

175   line analysis, we found that monkeys injected with the Cas9-MECP2 virus (n = 3) showed

176   decreased locomotor activity during the day compared to monkeys injected with the Cas9-Control

177   virus (n = 3) (Fig. 4A, B, C, D). To further measure the sleep patterns of the gene-edited monkeys,

178   activity data during the night (19:00 pm–07:00 am) were classified into awake and sleep phases,

179   with the sleep phase further divided into relaxed (no body movements during sleep) and

180   transitional (1–2 movements within 1 min) sleep phases (see Methods for definitions).

181

182   We found that durations of the awake and transitional sleep phases were significantly increased in

183   monkeys (n = 4) injected with the Cas9-MECP2 virus compared to monkeys injected with the

184   Cas9-Control virus (Fig. 4E, F). Consequently, the relaxed sleep period and overall sleep time

185   decreased in the Cas9-MECP2 virus-injected monkeys, but not in monkeys injected with the Cas9-

186   Control virus (Fig. 4G, 4H). Thus, sleep patterns were significantly fragmented in monkeys (e.g.,

187   #KO-3) injected with the Cas9-MECP2 virus (Fig. 4I). These abnormalities in sleep and activity

188   rhythms are similar to those observed in autistic patients [32, 37, 38] and to the phenotypes

189   identified in TALEN-edited *MECP2*-mutant cynomolgus monkeys [9].

190

191   **Defective social reward and communication behaviors in monkeys with *MECP2* deletions**

192   One prevalent hypothesis for the development of autistic-like behavioral abnormalities is that ASD

193   patients do not gain sufficient reward from social interaction, thereby leading to diminished

194   motivation for seeking or maintaining social contact [39]. Thus, we investigated whether social

195   reward is compromised by *MECP2* editing in the hippocampus using a monkey conditioned place

196   preference (CPP) paradigm [40] (Fig. S5, Table S1C). Briefly, monkeys underwent two

197   conditioning steps (i.e., social isolation and social interaction), followed by the choice to enter

198   either the isolation chamber (assigned based on previous color preference) or social chamber

199   (where a female partner was present during previous social conditioning). After social conditioning,

200   both groups of monkeys spent more time in the social cages than before (Fig. 5A, B). However,

201   the Cas9-Control monkeys (n = 3) spent more time in the social cages than the Cas9-MECP2

202   monkeys (n = 3), though without statistical significance (Fig. 5C, Movie S4, S5). These results

203   suggest that 3 d of social conditioning had a mild effect on the Cas9-MECP2 monkeys, but an

204   obvious effect on the Cas9-Control monkeys, supporting our speculation that deletion of *MECP2*

205 in the hippocampus compromises the social reward system, which may further aggravate social
206 interaction abnormalities in monkeys.

207

208 To further investigate social communication abilities, we observed the gaze-following behavior of
209 monkeys elicited by tracking the gaze of human experimenters [41]. Gaze-following is defined as
210 the ability of an individual to follow the direction of another's gaze. This ability is a critical process
211 through which social animals acquire necessary information on the emotional and mental states of
212 social partners. The age at which a human infant can follow the gaze of a caregiver ranges from 6
213 to 18 months, with monkeys also developing this ability during infancy [41, 42]. However,
214 children with ASD usually manifest developmental abnormality in gaze-following ability as a form
215 of social communication defect [42, 43]. Our results revealed that gaze-following responses in
216 monkeys (n = 2) decreased significantly following injection with the Cas9-MECP2 virus, but this
217 was not observed in the Cas9-Control monkeys (n = 2) (Fig. 5D, E, F, Movie S6, S7, Table S1D).
218 The Cas9-MECP2 group also showed significantly lower gaze-following than the Cas9-Control
219 group after virus injection (Cas9-MECP2 monkeys: n = 2, Cas9-Control monkeys: n = 2, Fig. 5G,
220 Movie S6, S7, Table S1D). The differences in gaze-following were not caused by different
221 interactions between the monkey and trainer as monkeys injected with either the Cas9-MECP2 or
222 Cas9-Control virus spent similar durations facing and looking at the trainer (Fig. S6A, B).

223

224 **Insensitivity for aversive sensory stimuli and lack of stereotypic behaviors in monkeys with**
225 *MECP2* **manipulations**
226 A common feature of ASD patients is their abnormal response to sensory stimuli (i.e., hyper- or
227 hypo-sensitivity), which can be a precipitating factor for deficits in social skills [44, 45]. To
228 determine whether *MECP2* gene editing in the hippocampus leads to defects in sensory responses,
229 we applied an active avoidance test to examine the auditory sensory responses of the monkeys [9].
230 The tested monkeys were placed in a shuttle box with two connected chambers, each equipped
231 with a high-pitch loudspeaker. High decibel white noise (116 dB) was played in the chamber
232 housing the tested monkey, which would normally trigger an escape response. Compared with the
233 Cas9-Control monkeys (n = 2), the Cas9-MECP2 monkeys (n = 2) became insensitive to noise
234 after virus injection (Fig. 6A, B, C, Movie S8, S9, Table S1E). Specifically, the Cas9-MECP2
235 group exhibited much longer escape time than the Cas9-Control group (Cas9-MECP2 monkeys: n

= 2, Cas9-Control monkeys: n = 2, Fig. 6D), suggesting that *MECP2* deletion in the hippocampus led to insensitivity to aversive sensory stimuli, thereby mimicking the sensory abnormalities of ASD patients. Interestingly, this result is similar to the abnormalities observed in whole-body TALEN-edited *MECP2*-mutant monkeys under the same procedure, suggesting that auditory sensory response abnormalities may be mediated by hippocampus-related neural circuitry [9].

Stereotypic and repetitive behaviors are core symptoms in ASDs and RTT[33]. Importantly, animal models based on *MECP2* mutation or duplication, including non-human primate models, exhibit various stereotypic behaviors [9, 26]. In the present study, however, stereotypic behaviors were not observed in monkeys injected with either the Cas9-MECP2 or Cas9-Control virus (Fig. 6E, F, Table S1A). These data suggest that manipulation of *MECP2* in the hippocampus specifically affects some aspects of social behavior and stereotypic behaviors may be regulated by the thalamic reticular system, as suggested previously [46]

Abnormal hand motions in monkeys with *MECP2* manipulations

Severe impairment in motor functions, especially abnormal hand motions, are primary components of Rett syndrome[31]. To examine whether *MECP2* gene editing in the brain causes motor disabilities in monkeys, we measured their physical mobility by the gait speed test (Fig. S7A) [47] and fine hand coordination by a modified brinkman board test (Fig. S7B) [48].No significant differences between the gene-edited and control groups were found in gait speed test, but there was significant difference in brinkman board test. Compare to control monkeys, gene-edited monkeys take longer times to retrieve a peanut kernel from designed slots, which showed the abnormal hand motions in gene-editing monkeys (Fig. S7A, B, Table S1F, Table S1G). Therefore, we concluded that down-regulation of the *MECP2* gene in the hippocampus will not cause postural dyskinesia, but will induce fine hand coordination disabilities in the rhesus monkeys.

***MECP2* edited monkeys may have learning and memory retrieval problems**

As Rett syndrome patients also exhibit severe impairment of cognitive functions, we performed two further behavioral tests to examine whether deletion of *MECP2* affects cognition and memory in monkeys. A reversal learning task was used to assess learning and cognitive flexibility and a modified pattern-recognition task was used to test memory [49, 50]. Although no statistical

267 differences were found between the Cas9-MECP2 (n = 3) and Cas9-Control monkeys (n = 2) in

268 these two tasks (Fig S8A, B, S9A-C, Table S1H-I), the Cas9-MECP2 monkeys needed more trials

269 to complete the learning phase and achieved a lower correct rate in the memory retrieval phase.

270 This evidence suggests that Cas9-MECP2 monkeys may have learning and memory retrieval

271 problems. Regrettably, due to the limitation of monkey numbers, the observed decline in cognition

272 and memory in the Cas9-MECP2 monkeys did not achieve a statistical conclusion. Thus, whether

273 down-regulation of the *MECP2* gene in the hippocampus causes impairment of cognition and

274 memory requires further study.

275

276 **MECP2 edited monkeys exhibited autistic-like phenotypes two years after gene-editing**

277 In order to examine the stability of the phenotype, longitudinal analysis was performed in the rest

278 of gene-editing and control monkeys. We analyzed social behaviors, light/dark activity, and sleep

279 patterns for 5 d on monkeys 2–3 years after gene-editing surgery (Table S4). As shown in the

280 following figures (Fig S10), we found that Cas9-MECP2 monkeys consistently exhibited social

281 deficit phenotypes, measured by duration of social interaction time and time monkeys spent alone

282 in comparison with Cas9-Control monkeys (Fig S10A). In the light/dark activity and sleep pattern

283 tests, we found that Cas9-MECP2 monkeys still showed increased transitional sleep and decreased

284 relaxed sleep compared to Cas9-Control monkeys. The day-time activity of Cas9-MECP2

285 monkeys also decreased compared to Cas-Control monkeys, consistent with the phenotypes (Fig

286 S10B). Therefore, we concluded that *in vivo* gene editing in monkey brains had lasting effects

287 regarding social behaviors, as well as circadian activities.

288

289 **Discussion**

290 We showed that AAV-delivered CRISPR/Cas9 gene editing efficiently induced deletion of

291 *MECP2* in the hippocampus of adolescent rhesus monkeys, which elicited core ASD-like

292 phenotypes, including defects in social communication and interaction, hyposensitivity to sensory

293 inputs, hypo-daytime activity, abnormal sleep patterns, abnormal hand motions and social reward

294 deficits. Thus, these results demonstrate that viral-based gene editing in a specific brain region can

295 be applied to rapidly develop monkey models that mimic ASD-like symptoms and shorten the

296 modelling cycle compared with traditional embryonic transgenic or gene editing strategies [9, 26].

297   This work is consistent with earlier studies demonstrating that deletion of *MECP2* in postmitotic
298   neurons in mice produces deficits in synaptic plasticity and RTT-like behaviors [51]. Furthermore,
299   we extended previous findings by revealing the essential role of hippocampal *MECP2* in the
300   regulation of social behaviors. Intriguingly, deletion of *MECP2* in the hippocampus of the
301   monkeys was not sufficient to recapitulate stereotypic behavior, which is observed in *MECP2*
302   transgenic and mutant monkeys [9, 26]. These results suggest that different brain areas have
303   different functions in ASDs and likely mediate distinct ASD symptoms. For example, specific
304   knockdown of *MECP2* in the basolateral amygdala can produce heightened anxiety-like behaviors
305   rather than abnormalities in social interaction [52]. This indicates that autistic-like symptoms could
306   be studied separately in different brain regions using our model, thus shedding light on the
307   connections between genes and specific neural circuitries.

308

309   Restoration of *Mecp2* during adulthood has been shown to rescue behavioral and physiological
310   defects in *Mecp2* knockout (KO) or overexpression (OE) mice [53-58]. The reason why defects
311   caused by loss of *MECP2* in the brain are reversible after birth may be due to the fact that MeCP2
312   regulates brain development through transcriptional repression, as well as regulation of microRNA
313   processing. Restoration of *Mecp2* to the normal level may be able to restore the impaired synaptic
314   plasticity in particular neural circuits by correction of abnormal gene expression caused by *loss*-
315   or *gain-of-function* of *Mecp2* in mouse models. The present findings suggest that the neural
316   circuitry responsible for social behaviors in non-human primates is also plastic and could be
317   manipulated during adolescence. The feasibility of postnatal social-circuit manipulation in
318   primates suggests a possible way to reverse autistic defects in human RTT and ASD patients.

319

320

Materials and Methods

Complete and detailed experimental procedures are provided in the supplementary materials

Experimental Design

This study aimed to improve the feasibility of inducing ASD models in wild-type monkeys in order to fulfil the large production demands of disease and drug screening studies. Thus, we induced genetic mutations of the ASD-related gene *MECP2* in the hippocampus of adult rhesus macaques *in vivo* via adeno-associated virus (AAV9)-delivered *Staphylococcus aureus* Cas9. Through behavioral analysis, our model successfully mimicked the symptoms of ASD disease, thus paving the way for the rapid generation of genetically engineered non-human primate models for neurobiological studies and therapeutic development.

Animals and ethics

Eleven young healthy male rhesus macaques (*Macaca mulatta*) (3–5 kg, 2–3 years old) from the Kunming Primate Research Center of the Chinese Academy of Sciences were used in this study. All monkeys were treated in accordance with the National Institute of Health's (USA) Guide for the Care and Use of Laboratory Animals [59]. All animals had continuous access to water and monkey chow supplemented with seasonal fresh fruit and/or vegetables. The animals lived in their respective social groups (6–8 male monkeys of similar age) for at least five months prior to the experiments. They were transferred to individual cages ($0.74 \times 0.71 \times 0.74$ m) after operation for recovery and individual behavioral assessment under normal conditions (temperature 21 ± 2 ℃, 14/10 h light/dark cycle, light from 07:00 am to 19:00 pm, relative humidity 60%, with standard monkey chow and daily fruit). All experimental protocols and animal care and handling were approved by the Ethics Committee of the Kunming Institute of Zoology and Kunming Primate Research Center (NO. IACUC18019), Chinese Academy of Sciences (AAALAC accredited).

MRI-guided hippocampus localization

The MRI-guided hippocampus localization procedure was adapted from our previous study [29]. Briefly, two rigid glass tubes (3–4 cm long, internal diameter 0.5 mm, external diameter 0.9 mm) were filled with glycerol to serve as markers, appearing as a high signal in the MRI (T2) images.

352   The markers were fixed onto the skull by dental cement according to stereotaxic coordinates: i.e.,

353   anterior-posterior +10 mm and medial-lateral ±10 mm. After operation, the monkeys were sent for

354   MRI scanning [(1) Siemens Avanto 1.5T scanner (Siemens, Erlangen, Germany), 3D FLASH (fast

355   low-angle shot) spoiled gradient-echo sequence, slice 1.0 mm, distance factor 0.2 mm/20%, FOV

356   150 × 122 mm, resolution 320 × 320, TR 13.0 ms, TE 5.07 ms, average 3. (2) UIH uMR770 3T

357   scanner (United Imaging, Shanghai, China), 3D five-echo GRE sequence, slice = 0.8 mm, distance

358   factor 0.1 mm/10%, FOV = 124 × 124 mm, resolution 320 × 320, TR = 2300 ms, TE = 380 ms,

359   average 2]. The size of the hippocampus and its relative location to the glycerol markers were

360   calculated using the MRI images (Fig. S1). The injection pathways and volumes were then

361   determined according to the injection coordinates for each monkey listed in Table S2.

362

Viral vector design and AAV production

364   The AAV-SaCas9 vector was obtained from Addgene (RRID: Addgene_61593). The TBG

365   promoter was replaced with human synapsin promoter for better expression in the brain. The

366   sgRNAs were annealed from DNA oligos with BsaI digest ends. After annealing, the sgRNA

367   segments were inserted into the BsaI site of the vector. The AAV9 (AAV-hSyn-SaCas9-U6-

368   sgMECP2-a titer = 1.12 E + 13 V.G./mL; AAV-hSyn-SaCas9-U6-sgMECP2-b titer = 1.64 E + 13

369   V.G./mL; AAV-hSyn-SaCas9-U6-sgLacZ titer = 1.56 E + 13 V.G./mL; AAV-hSyn-GFP titer =

370   2.18E + 13 V.G./mL) was constructed at the ION Virus Production Core Facility (Shanghai,

371   China).

372

Statistical analysis

374   Data analysis was conducted using GraphPad Prism v8.00 (GraphPad Software, La Jolla,

375   California, USA), SPSS v19.0 (SPSS, Chicago, IL, USA) and R (version 3.3.2) for Windows.

376   Mann Whitney tests were applied for intragroup analysis. Repeated-measures analysis of variance

377   (ANOVA) was used for intergroup analysis. For modified brinkman board test, the effect of group,

378   size and size-by-group interactions of brinkman score were assessed using a general linear model

379   (GLM) with the following equation: dependent variable (brinkman) = Intercept +group + size +

380   group×size+ random error. The group effect p values by corrections for multiple tests were

381   conducted using Bonferroni. Data are means ± SEM, * $p < 0.05$, ** $p < 0.01$, *** $p < 0.001$.

382

References and Notes

1. Jinek, M., et al., *A programmable dual-RNA–guided DNA endonuclease in adaptive bacterial immunity.* science, 2012: p. 1225829.
2. Mali, P., et al., *RNA-guided human genome engineering via Cas9.* Science, 2013. **339**(6121): p. 823-826.
3. Cong, L., et al., *Multiplex genome engineering using CRISPR/Cas systems.* Science, 2013: p. 1231143.
4. Ran, F.A., et al., *In vivo genome editing using Staphylococcus aureus Cas9.* Nature, 2015. **520**(7546): p. 186.
5. Li, D.L., et al., *Heritable gene targeting in the mouse and rat using a CRISPR-Cas system.* Nat Biotechnol, 2013. **31**(8): p. 681-683.
6. Wang, H.Y., et al., *One-step generation of mice carrying mutations in multiple genes by CRISPR/Cas-mediated genome engineering.* Cell, 2013. **153**(4): p. 910-918.
7. Liu, H., et al., *TALEN-mediated gene mutagenesis in rhesus and cynomolgus monkeys.* Cell stem cell, 2014. **14**(3): p. 323-328.
8. Liu, Z., et al., *Generation of a monkey with MECP2 mutations by TALEN-based gene targeting.* Neuroscience bulletin, 2014. **30**(3): p. 381-386.
9. Chen, Y., et al., *Modeling Rett Syndrome Using TALEN-Edited MECP2 Mutant Cynomolgus Monkeys.* Cell, 2017. **169**(5): p. 945-955 e10.
10. Niu, Y., et al., *Generation of Gene-Modified Cynomolgus Monkey via Cas9/RNA-Mediated Gene Targeting in One-Cell Embryos.* Cell, 2014. **156**(4): p. 836-843.
11. Yao, X., et al., *Generation of knock-in cynomolgus monkey via CRISPR/Cas9 editing.* Cell Research, 2018. **28**(3): p. 379-382.
12. Kang, Y., et al., *CRISPR/Cas9-mediated genome editing in nonhuman primates.* Dis Model Mech, 2019. **12**(10).
13. Chen, Y., et al., *Functional disruption of the dystrophin gene in rhesus monkey using CRISPR/Cas9.* Human Molecular Genetics, 2015: p. 120.
14. Kang, Y., et al., *CRISPR/Cas9-mediatedDax1 knockout in the monkey recapitulates human AHC-HH.* Human Molecular Genetics, 2015: p. 24.
15. Tu, Z., et al., *CRISPR/Cas9-mediated disruption of SHANK3 in monkey leads to drug-treatable autism-like symptoms.* Hum Mol Genet, 2019. **28**(4): p. 561-571.
16. Zhou, Y., et al., *Atypical behaviour and connectivity in SHANK3-mutant macaques.* Nature, 2019. **570**(7761): p. 326-331.
17. Xue, W., et al., *CRISPR-mediated direct mutation of cancer genes in the mouse liver.* Nature, 2014. **514**(7522): p. 380.
18. Long, C., et al., *Postnatal genome editing partially restores dystrophin expression in a mouse model of muscular dystrophy.* Science, 2016. **351**(6271): p. 400-403.
19. Nelson, C.E., et al., *In vivo genome editing improves muscle function in a mouse model of Duchenne muscular dystrophy.* Science, 2016. **351**(6271): p. 403-407.
20. Tabebordbar, M., et al., *In vivo gene editing in dystrophic mouse muscle and muscle stem cells.* Science, 2016. **351**(6271): p. 407-411.
21. Yang, W., et al., *Mutant alpha-synuclein causes age-dependent neuropathology in monkey brain.* J Neurosci, 2015. **35**(21): p. 8345-58.

453 22. Eslamboli, A., et al., *Long-term consequences of human alpha-synuclein overexpression
454   in the primate ventral midbrain.* Brain, 2007. **130**(Pt 3): p. 799-815.
455 23. Kirik, D., et al., *Nigrostriatal alpha-synucleinopathy induced by viral vector-mediated
456   overexpression of human alpha-synuclein: a new primate model of Parkinson's disease.*
457   Proc Natl Acad Sci U S A, 2003. **100**(5): p. 2884-9.
458 24. Nan, X.S., F.J. Campoy, and A. Bird, *MeCP2 is a transcriptional repressor with abundant
459   binding sites in genomic chromatin.* Cell, 1997. **88**(4): p. 471-481.
460 25. Amir, R.E., et al., *Rett syndrome is caused by mutations in X-linked MECP2, encoding
461   methyl-CpG-binding protein 2.* Nature genetics, 1999. **23**(2): p. 185.
462 26. Liu, Z., et al., *Autism-like behaviours and germline transmission in transgenic monkeys
463   overexpressing MeCP2.* Nature, 2016. **530**(7588): p. 98-102.
464 27. Hitti, F.L. and S.A. Siegelbaum, *The hippocampal CA2 region is essential for social
465   memory.* Nature, 2014. **508**(7494): p. 88-92.
466 28. Okuyama, T., et al., *Ventral CA1 neurons store social memory.* Science, 2016. **353**(6307):
467   p. 1536.
468 29. Jing, W., et al., *A new MRI approach for accurately implanting microelectrodes into deep
469   brain structures of the rhesus monkey (Macaca mulatta).* Journal of neuroscience methods,
470   2010. **193**(2): p. 203-209.
471 30. Wu, S.H., et al., *Comparative study of the transfection efficiency of commonly used viral
472   vectors in rhesus monkey (Macaca mulatta) brains.* Zool Res, 2017. **38**(2): p. 88-95.
473 31. Hagberg, B., et al., *An update on clinically applicable diagnostic criteria in Rett syndrome.
474   Comments to Rett Syndrome Clinical Criteria Consensus Panel Satellite to European
475   Paediatric Neurology Society Meeting, Baden Baden, Germany, 11 September 2001.* Eur
476   J Paediatr Neurol, 2002. **6**(5): p. 293-7.
477 32. Mazzone, L., et al., *The Relationship between Sleep Problems, Neurobiological Alterations,
478   Core Symptoms of Autism Spectrum Disorder, and Psychiatric Comorbidities.* Journal of
479   Clinical Medicine, 2018. **7**(5): p. 102.
480 33. Dilip V. Jeste, R.S.B., M elinda L. Young, *Diagnostic and statistical manual of mental
481   disorders: DSM-5™ (5th ed.).* American Psychiatric Association, 2013(2): p. 50.
482 34. Maïano, C., et al., *Prevalence of School Bullying Among Youth with Autism Spectrum
483   Disorders: A Systematic Review and Meta-Analysis.* Autism Research, 2015. **9**(6): p. 601-
484   615.
485 35. Mccoy, S.M., J.M. Jakicic, and B.B. Gibbs, *Comparison of Obesity, Physical Activity, and
486   Sedentary Behaviors Between Adolescents With Autism Spectrum Disorders and Without.*
487   Journal of Autism & Developmental Disorders, 2016. **46**(7): p. 1-10.
488 36. P, K., et al., *Sleep problems in children with autism spectrum disorders, developmental
489   delays, and typical development: a population-based study.* Journal of Sleep Research,
490   2012. **21**(2): p. 197-206.
491 37. Humphreys, J.S., et al., *Sleep patterns in children with autistic spectrum disorders: a
492   prospective cohort study.* Archives of Disease in Childhood, 2014. **99**(2): p. 114-8.
493 38. Li, Q., et al., *Circadian rhythm disruption in a mouse model of Rett syndrome circadian
494   disruption in RTT.* Neurobiology of disease, 2015. **77**: p. 155-164.
495 39. Chevallier, C., et al., *The social motivation theory of autism.* Trends Cogn Sci, 2012. **16**(4):
496   p. 231-9.
497 40. Dölen, G., et al., *Social reward requires coordinated activity of nucleus accumbens
498   oxytocin and serotonin.* Nature, 2013. **501**(7466): p. 179.

499 41. Ferrari, P.F., et al., *The ability to follow eye gaze and its emergence during development in macaque monkeys.* Proc Natl Acad Sci U S A, 2000. **97**(25): p. 13997-4002.

501 42. NJ, E., *The eyes have it: the neuroethology, function and evolution of social gaze.* Neuroscience and Biobehavioral Reviews, 2000. **24**(6): p. 581-604.

503 43. Baroncohen, S., et al., *Are children with autism blind to the mentalistic significance of the eyes?* British Journal of Developmental Psychology, 2011. **13**(4): p. 379-398.

505 44. Takahashi, H., et al., *Relationship of the Acoustic Startle Response and Its Modulation to Emotional and Behavioral Problems in Typical Development Children and Those with Autism Spectrum Disorders.* Journal of Autism & Developmental Disorders, 2015. **46**(2): p. 1-10.

509 45. Lucker, J.R., *Auditory Hypersensitivity in Children with Autism Spectrum Disorders.* Focus on Autism & Other Developmental Disabilities, 2013. **28**(3): p. 184-191.

511 46. Krol, A., et al., *Thalamic Reticular Dysfunction as a Circuit Endophenotype in Neurodevelopmental Disorders.* Neuron, 2018. **98**(2): p. 282–295.

513 47. Shively, C.A., et al., *Aging and physical mobility in group-housed Old World monkeys.* **34**(5): p. 1123-1131.

515 48. Schmidlin, E., et al., *Behavioral assessment of manual dexterity in non-human primates.* J Vis Exp, 2011(57).

517 49. Izquierdo, A., et al., *The neural basis of reversal learning: An updated perspective.* 2016. **345**: p. 12-26.

519 50. Mishkin, M. and T. Appenzeller, *The anatomy of memory.* 1987. **256**(6): p. 80-9.

520 51. McGraw, C.M., R.C. Samaco, and H.Y. Zoghbi, *Adult neural function requires MeCP2.* Science, 2011. **333**(6039): p. 186.

522 52. Adachi, M., et al., *MeCP2-Mediated Transcription Repression in the Basolateral Amygdala May Underlie Heightened Anxiety in a Mouse Model of Rett Syndrome.* Journal of Neuroscience, 2009. **29**(13): p. 4218-4227.

525 53. Luikenhuis, S., et al., *Expression of MeCP2 in postmitotic neurons rescues Rett syndrome in mice.* Proc Natl Acad Sci U S A, 2004. **101**(16): p. 6033-8.

527 54. Guy, J., et al., *Reversal of neurological defects in a mouse model of Rett syndrome.* Science, 2007. **315**(5815): p. 1143-1147.

529 55. Tillotson, R., et al., *Radically truncated MeCP2 rescues Rett syndrome-like neurological defects.* Nature, 2017. **550**(7676): p. 398.

531 56. Sztainberg, Y., et al., *Reversal of phenotypes in MECP2 duplication mice using genetic rescue or antisense oligonucleotides.* Nature, 2015. **528**(7580): p. 123-126.

533 57   c, L.S.a., et al., Visualization and correction of social abnormalities-associated neural ensembles in adult MECP2 duplication mice. Science Bulletin, 2020. **65**(14): p. 1192-1202.

535 58   Yu, B., et al., Reversal of Social Recognition Deficit in Adult Mice with MECP2 Duplication via Normalization of MeCP2 in the Medial Prefrontal Cortex. Neuroscience Bulletin, 2020. **36**(6): p.570-584.

538 59. Janet C. Garber, R.W.b., Joseph T. bielitzki, Leigh Ann Clayton, *Guide for the care and use of laboratory animals.* 2011: THE NATIONSL ACADEMIES.

540

541

542

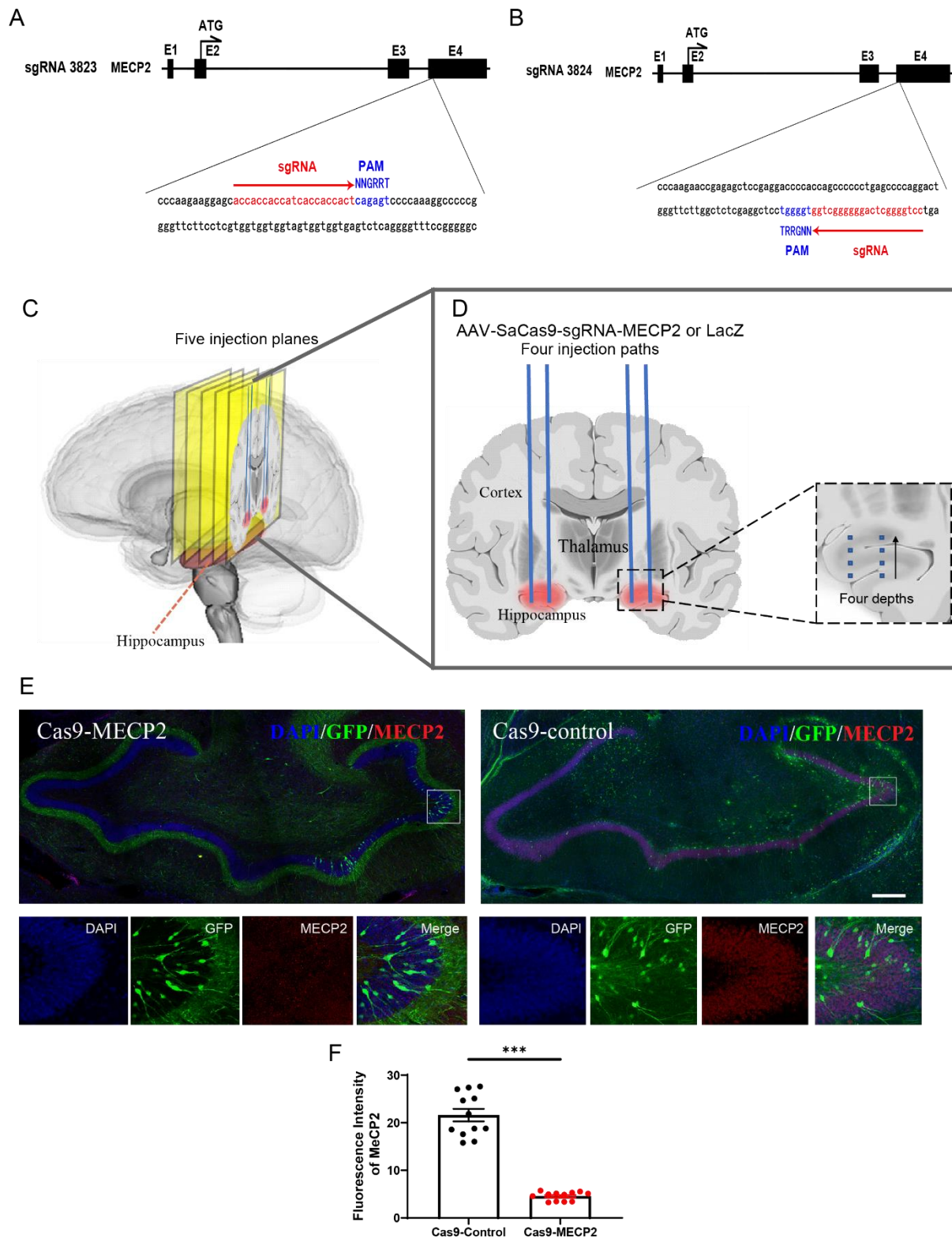543 **Figures and Tables**

Figure 1.

544

545 **Figure 1. Design of sgRNAs for SaCas9, injection protocols, and validation *in vivo*.**

546 (**A-B**) Targeting sites of sgRNA for monkey *MECP2* gene. PAM sequences are in blue.

547 sgRNA-MECP2-a was designed according to PAM sequence on plus stand and sgRNA-

548 MECP2-b was designed according to PAM sequence on minus stand. (**C-D**) Schematic of

549 injection strategy for monkey KO-2, location of hippocampus was determined by MRI

550 images. Five injection planes were selected for viral injections from anterior to posterior

551 to cover entire hippocampus. There were two injection paths in every injection plane on

552 each side of the hippocampus. Injections were given at four different depth sites along each

553 injection path. Details of injection strategy are provided in the Supplementary Materials.

554 (**E**) Immunostaining of hippocampal sections of Cas9-MECP2 (KO-3) and Cas9-Control

555 (Ctrl-2) monkeys for GFP (green), MECP2 (red), and DAPI (blue). Scale bar, 500 μm. (**F**)

556 Arbitrary units for fluorescence intensity of MECP2 protein signals in DAPI-positive cells

557 detected by anti-MECP2 antibody were quantified (n = 12, from two monkeys of each

558 group, Cas9-Control: Ctrl-1 and Ctrl-2, Cas9-MECP2: KO-3 and KO-7). Fluorescence

559 signal of MECP2 proteins was reduced in Cas9-MECP2 monkeys (Mann-Whitney test, U
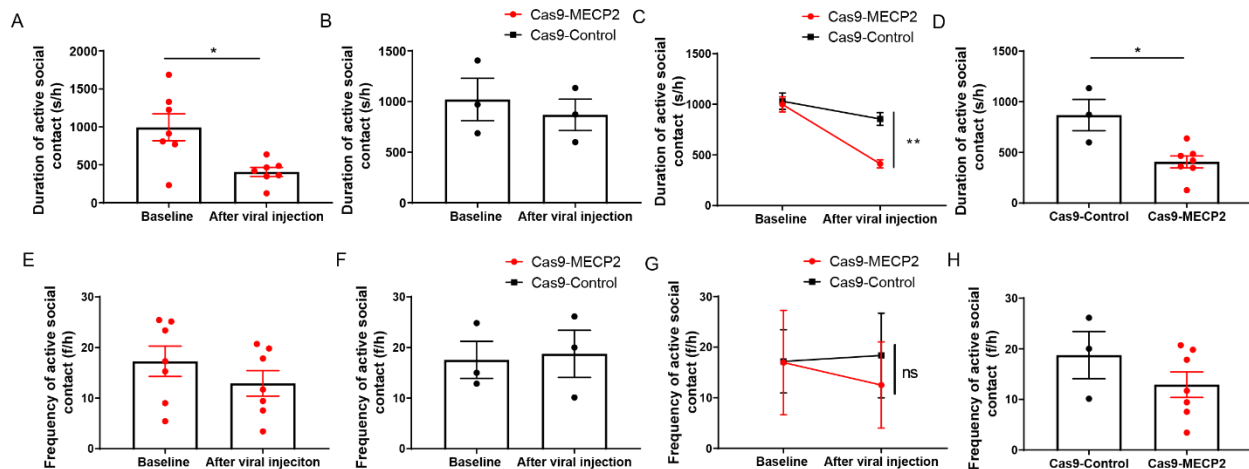
560 = 0, *** $p < 0.0001$).

561

Figure 2.

Figure 2. Monkeys with acute *MECP2* gene editing exhibited abnormal social behaviors. (**A**) Duration of social contact in Cas9-MECP2 group (Mann-Whitney test, U = 6, * p = 0.0175, n = 7, from seven monkeys, average of 7 d of repeated measurements per monkey) and (**B**) Cas9-Control group before and after injection (n = 3, from three monkeys, average of 7 d of repeated measurements per monkey). (**C**) Changes in active social contact after injection were significantly different between Cas9-MECP2 and Cas9-Control groups (repeated-measures ANOVA, F = 8.245, ** p = 0.005, η_p^2 = 0.111). (**D**) Cas9-MECP2 group (n = 7) showed significantly shorter duration of active social contact compared to Cas9-Control group (n = 3) after injection (Mann-Whitney test, U = 1, * p = 0.0333). (**E**) Frequency of social contact in Cas9-MECP2 group (n = 7, from seven monkeys, average of 7 d of repeated measurements per monkey) and Cas9-Control group (**F**) (n = 3, from three monkeys, average of 7 d of repeated measurements per monkey). (**G**) No significant differences in frequency were found between groups (repeated-measures ANOVA, p = 0.115). (**H**) Cas9-MECP2 group (n = 7) showed similar frequency of active social contact as Cas9-Control group (n = 3) after injection. Each spot represents average duration time of social contact (7 d) for individual monkeys during daily observation periods. Data are means ± SEM, data within 95% confidence interval were included in statistical analysis.
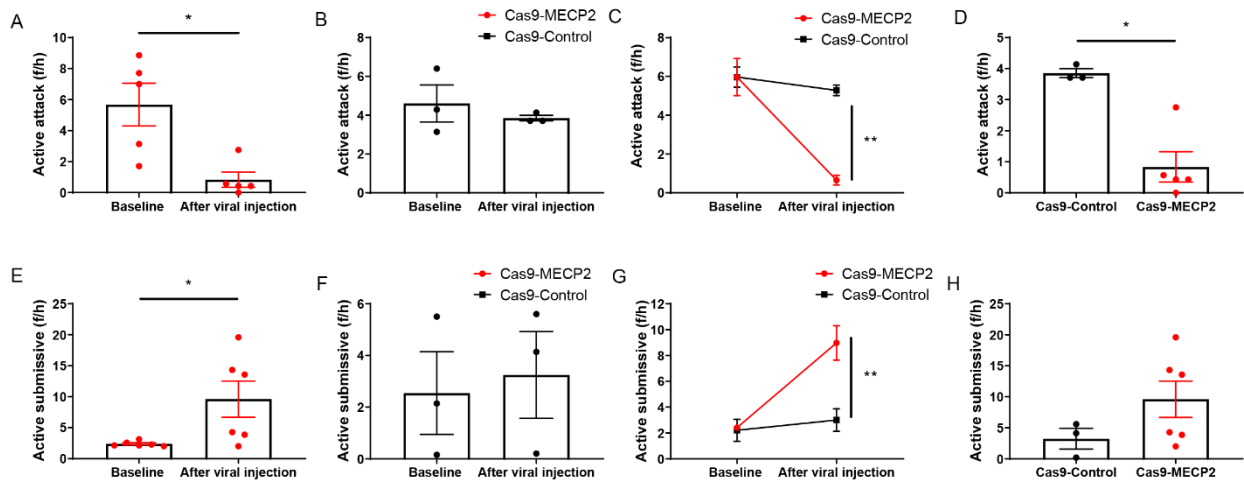
581

Figure 3.

Figure 3. Monkeys with acute *MECP2* gene editing exhibited abnormal aggressive behaviors. (**A**) Active attacks decreased in Cas9-MECP2 group (n = 5, from five monkeys, average of 7 d of repeated measurements per monkey) after injection (Mann-Whitney test, U = 1, * p = 0.0159), (**B**) but not in Cas9-Control group (n = 3, from three monkeys, average of 7 d of repeated measurements per monkey). (**C**) Changes in active attacks after injection were significantly different between Cas9-MECP2 and Cas9-Control groups (repeated-measures ANOVA, F = 12.232, ** p = 0.0010, η_p^2 = 0.200). (**D**) Cas9-MECP2 group (n = 5) showed significantly lower active attacks than Cas9-Control group (n = 3) after injection (Mann-Whitney test, U = 0, * p = 0.0357). (**E**) Submissive behaviors increased in Cas9-MECP2 group after injection (n = 6, from six monkeys, average of 7 d of repeated measurements per monkey, Mann-Whitney test, U = 5.5, * p = 0.0476), (**F**) but not in Cas9-Control group (n = 3, from three monkeys, average of 7 d of repeated measurements per monkey). (**G**) Changes in submissive behaviors were significantly different between Cas9-MECP2 and Cas9-Control groups (repeated-measures ANOVA, F = 8.022, ** p = 0.006, η_p^2 = 0.125). (**H**) Cas9-MECP2 group (n = 6) displayed more submissive behaviors than Cas9-Control group (n = 3) after injections. Each dot indicates average time (7 d) of social activity for individual monkeys during daily observation period. Data are means ± SEM, data within 95% confidence interval were included in statistical analysis.
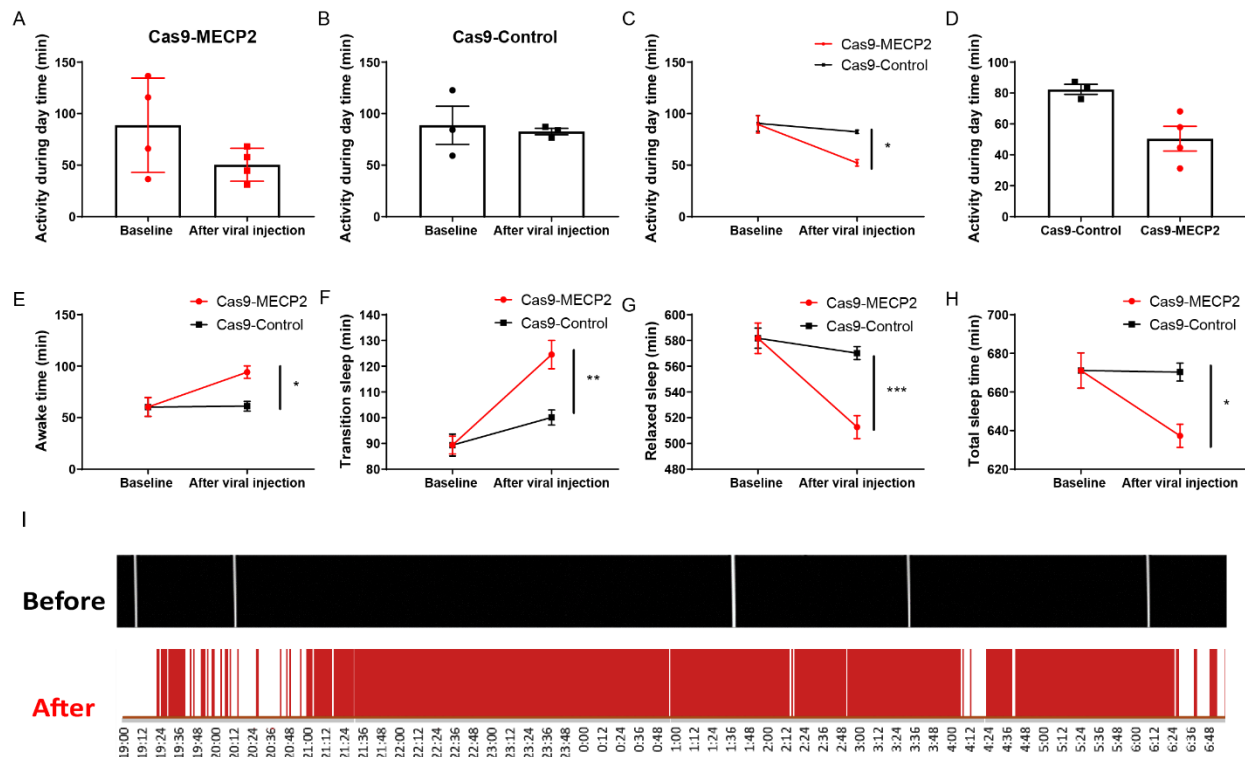
601

Figure 4.

602

Figure 4. Hypoactivity and abnormal sleep patterns in acute *MECP2* gene-edited monkeys. (**A**) Cas9-MECP2 (n = 4, from four monkeys, average of 7 d of repeated measurements per monkey) and (**B**) Cas9-Control groups (n = 3, from three monkeys, average of 7 d of repeated measurements per monkey) exhibited no significant changes in daytime activity. (**C**) Changes in daytime activity after viral injection were significantly different between Cas9-MECP2 and Cas9-Control groups (repeated-measures ANOVA, F = 6.782; * p = 0.013; η_p^2 = 0.136). (**D**) After viral injection, Cas9-MECP2 group showed shorter daytime activity compared with Cas9-Control group. (**E**) Cas9-MECP2 group showed significantly increased awake time duration after injection compared with control group (repeated-measures ANOVA, F = 6.782; * p = 0.012, η_p^2 = 0.126; Cas9-MECP2 group, n = 28, from 7 d of measurements of four monkeys; Cas9-Control group, n = 21 from 7 d of measurements of three monkeys). (**F**) Cas9-MECP2 group showed significantly increased duration of transitional sleep compared with control group (repeated-measures ANOVA, F = 10.6, ** p = 0.002, η_p^2 = 0.184; Cas9-MECP2 group, n = 28, from 7 d of measurements of four monkeys; Cas9-Control group, n = 21 from 7 d of measurements of

618   three monkeys). (**G**) Cas9-MECP2 group exhibited significantly decreased duration of

619   relaxed sleep compared with control group (repeated-measures ANOVA, F = 14.04; *** p

620   < 0.0001, η_p^2 = 0.23; Cas9-MECP2 group, n = 28, from 7 d of measurements of four

621   monkeys; Cas9-Control group, n = 21, from 7 d of measurements of three monkeys). (**H**)

622   Cas9-MECP2 group exhibited significantly decreased duration of total sleep compared

623   with control group (repeated-measures ANOVA, F = 6.782, * p = 0.012; η_p^2 = 0.126; Cas9-

624   MECP2 group, n = 28, from 7 d of measurements of four monkeys; Cas9-Control group, n

625   = 21 from 7 d of measurements of three monkeys). (**I**) Two examples of sleep patterns (12

626   h from 19:00 pm to 07:00 am) from same monkey (KO-3), illustrating fragmented sleep

627   after gene editing. Each dot (in **A, B, D**) indicates average of 7 d activity of individual

628   monkeys during 12-h daily observation period (07:00 am–19:00 pm, 7 d). Data are means
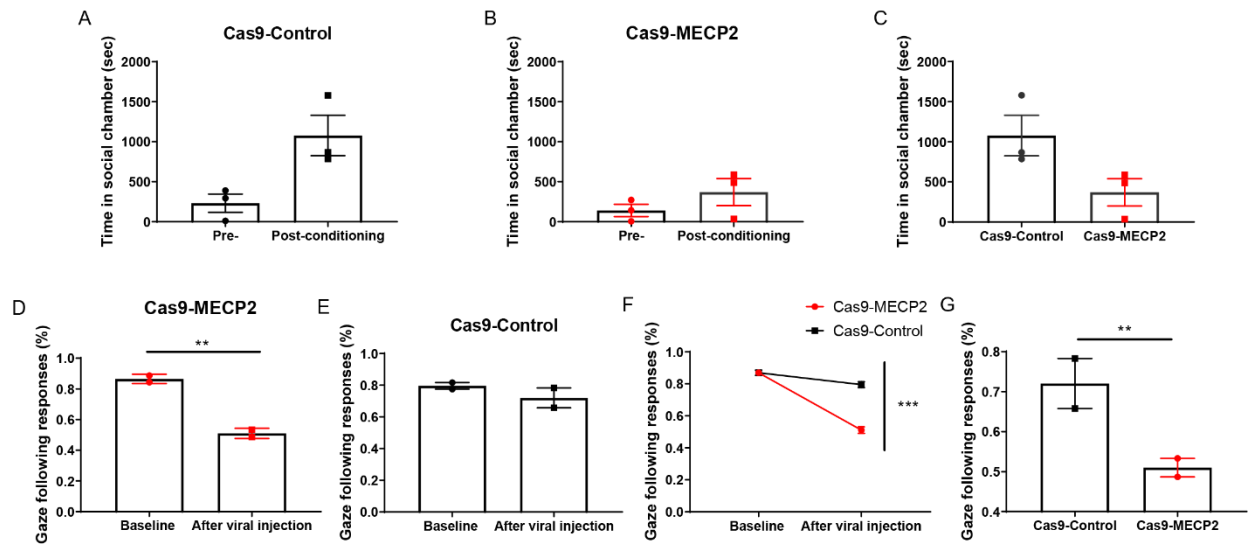
629   ± SEM.

630

631

632

Figure 5.

633

Figure 5. Monkeys with *MECP2* gene editing exhibited deficits in social reward and gaze following. After isolation and social conditioning, (**A**) Cas9-Control (n = 3 monkeys) and (**B**) Cas9-MECP2 groups (n = 3 monkeys) exhibited no significant changes in duration in social chamber. (**C**) Compared to Cas9-MECP2 group, Cas9-Control group spent more time in social chamber, revealing possible deficits in social reward function. (**D**) Cas9-MECP2 group showed significantly decreased gaze-following after virus injection (Mann-Whitney test, U = 0, ** p = 0.0022, n = 6, from 3 d of measurements of two monkeys). (**E**) Cas9-Control group exhibited no significant changes in gaze-following responses (n = 6, from 3 d of measurements of two monkeys). (**F**) Changes in gaze-following rate were significantly different between Cas9-MECP2 and Cas9-Control groups (repeated-measures ANOVA, F = 21.114, *** p = 0.001, η_p^2 = 0.679). (**G**) Cas9-MECP2 group showed significantly lower gaze-following rate than Cas9-Control group after viral injection (Mann-Whitney test, U = 1, ** p = 0.0022). (**A, B**) Each dot indicates duration of individual monkeys in social chamber during 30-min testing period, and (**D, E, G**) each dot indicates average percentage of gaze-following of individual monkeys during 3-d test period. Data are means ± SEM.
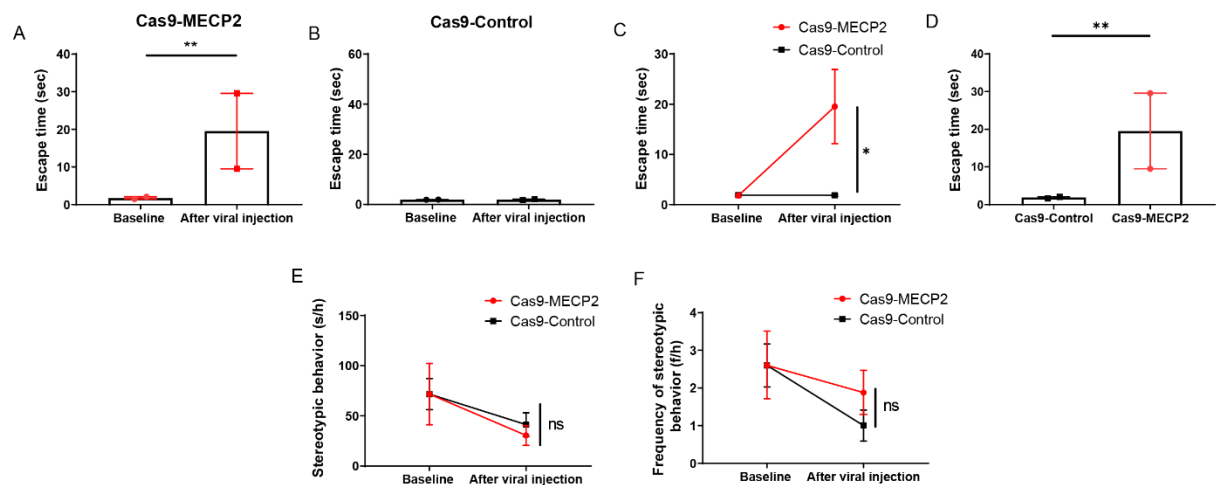
650

651

Figure 6.

652

653 **Figure 6. Monkeys with *MECP2* gene editing exhibited abnormal responses to**
654 **aversive sensory stimuli and unchanged repetitive behaviors.** (**A**) After injection, Cas9-
655 MECP2 group showed significantly increased escape latency from noise chamber in active
656 avoidance test (Mann-Whitney test, U = 0, ** p = 0.0022, n = 6, from 3 d of measurements
657 of two monkeys). (**B**) Cas9-Control group exhibited no change in escape latency (n = 6,
658 from 3 d of measurements of two monkeys). (**C**) Changes in both groups were significantly
659 different (repeated-measures ANOVA, F = 5.644, * p = 0.039, η_p^2 = 0.361; Cas9-MECP2,
660 n = 6; Cas9-Control, n = 6). (**D**) Cas9-MECP2 group exhibited significantly longer escape
661 latency than Cas9-Control group after injection (Mann-Whitney test, U = 0, ** p = 0.0022).
662 Duration (**E**) and frequency (**F**) of stereotypic behaviors exhibited no significant changes
663 in Cas9-MECP2 and Cas9-Control groups (repeated-measures ANOVA, E: p = 0.833, F:
664 p = 0.29). (**A, B, D**) Each dot indicates average escape latency of individual monkeys
665 during 3-d observation period. Data are means ± SEM.

666

667 **Supplementary Materials**

668

669   1.Supplemental Experimental Procedures

670   2.Figures S1 to S9

671   3.Tables S1 to S3

672   4. Movie details

673   5.Supplemental References

674

675 **Experimental procedures**

676

677 **Animals and ethics**

678 Eleven young healthy male rhesus macaques (*Macaca mulatta*) (3–5 kg, 2–3 years old) from the

679 Kunming Primate Research Center of the Chinese Academy of Sciences were used for this study.

680 All monkeys were treated in accordance with the National Institute of Health's (USA) Guide for

681 the Care and Use of Laboratory Animals [1]. All animals had continuous access to water and

682 monkey chow supplemented with seasonal fresh fruit and/or vegetables. All animals lived in their

683 respective social groups (6–8 male monkeys of similar age) for at least five months prior to the

684 experiments. They were transferred to individual cages ($0.74 \times 0.71 \times 0.74$ m) after operation for

685 recovery and individual behavioral assessment under normal conditions (temperature 21 ± 2 ℃,

686 14/10 h light/dark cycle, light from 07:00 am to 19:00 pm, relative humidity 60%, with standard

687 monkey chow and daily fruit). All experimental protocols and animal care and handling were

688 approved by the Ethics Committee of the Kunming Institute of Zoology and Kunming Primate

689 Research Center (NO. IACUC18019), Chinese Academy of Sciences (AAALAC accredited).

690

691 **MRI-guided hippocampal localization**

692 The MRI-guided hippocampal localization procedure was adapted from our previous study [2].

693 Briefly, two rigid glass tubes (3–4 cm long, internal diameter 0.5 mm, external diameter 0.9 mm)

694 were filled with glycerol to serve as markers, appearing as a high signal in the MRI (T2) images.

695 The markers were fixed onto the skull with dental cement according to stereotaxic coordinates:

696 i.e., anterior-posterior +10 mm and medial-lateral ±10 mm. After operation, the monkeys were

697 sent for MRI scanning. [(1) Siemens Avanto 1.5T scanner (Siemens, Erlangen, Germany), 3D

698 FLASH (fast low-angle shot) spoiled gradient-echo sequence, slice 1.0 mm, distance factor 0.2

699 mm/20%, FOV 150×122 mm, resolution 320×320, TR 13.0 ms, TE 5.07 ms, average 3. (2) UIH

700 uMR770 3T scanner (United Imaging, Shanghai, China), 3D five-echo GRE sequence, slice = 0.8

701 mm, distance factor 0.1 mm/10%, FOV = 124×124 mm, resolution 320×320, TR = 2300 ms,

702 TE = 380 ms, average 2]. The size of the hippocampus and its relative location to the glycerol

703 markers were calculated using the MRI images (Fig. S1). The injection pathways and virus

704 volumes were then determined according to the injection coordinates for each monkey listed in

705 Table S2.

706

Viral vector design and AAV production

708 The AAV-SaCas9 vector was obtained from Addgene (#61593). The TBG promoter was replaced

709 with human synapsin promoter for better expression in the brain. The sgRNAs were annealed from

710 DNA oligos with BsaI digest ends. After annealing, the sgRNA segments were inserted into the

711 BsaI site of the vector. The AAV viruses (AAV-hSyn-SaCas9-U6-sgMECP2-a titer = 1.12 E + 13

712 V.G./mL; AAV-hSyn-SaCas9-U6-sgMECP2-a titer = 1.64 E + 13 V.G./mL; AAV-hSyn-GFP titer

713 = 2.18E + 13 V.G./mL) were constructed at the ION Virus Production Core Facility (Shanghai,

714 China).

715

AAV injections

717 Prior to surgery, all monkeys were anesthetized with atropine (SFDA approval number:

718 H41021257, 0.03–0.05 mg/kg, i.m.), and then injected with ketamine (Veterinary Drug approval

719 number (2015)100761663, 10 mg/kg, i.m.) and pentobarbital (Merck, 40 mg/kg, i.m.). All surgical

720 procedures were conducted under strict aseptic conditions. As a prophylactic antibiotic treatment,

721 cephalosporin (SFDA approval number: H23021439) was injected for five consecutive days after

722 surgery (25 mg/kg/day, i.m, once a day). Each monkey's head was fixed on an RWD stereotaxic

723 frame (Product Model: 68902, Shenzhen, China) and a craniotomy was carried out by dental

724 drilling according to the stereotaxic coordinates obtained from MRI scanning. The virus was then

725 infused through a 31-gauge Hamilton syringe placed in a syringe pump (WPI Apparatus, Sarasota,

726 USA) at a speed of 800 nL/min. After infusion, the needle was left in place for 8 min before being

727 slowly retracted from the brain. The same operation was repeated until all injections were finished.

728 After injection, the wound was cleaned thoroughly and sutured [3].

729

Immunohistochemistry

731 Monkeys were anesthetized with pentobarbital (45 mg/kg, i.m) and transcardially perfused with

732 2000 mL of 4 °C phosphate-buffered saline (PBS) and 500 mL of 4% paraformaldehyde (Sigma-

733 Aldrich, Cat# 16005) in PBS. After perfusion, the hemispheres of the brain were dissected, cut

734 into small blocks, fixed with 4% paraformaldehyde in PBS, and equilibrated in 30% sucrose. The

735 fixed and equilibrated brain tissue blocks were then cut into 50-μm cortical sections with a Microm

736 HM525 cryostat (Microm, Walldorf, Germany). Sections were washed for 5 min in PBS

737   containing 5% bovine serum albumin (BSA) and 0.3% Triton X-100, and incubated with primary

738   antibodies (in PBS with 1% BSA and 0.3% Triton X-100) overnight at 4 °C and subsequently with

739   corresponding secondary antibodies (Alexa-Fluor-conjugated, Invitrogen, at 1:1000). DAPI was

740   used to label the nuclei and sections were mounted with 75% glycerol. Other antibodies used

741   included: GFP antibody (Abcam, ab6673), MeCP2 antibody (Cell Signaling, 3456S), anti-GFAP

742   (1:800; Biolegend, SMI-21R), and anti-Iba1 (1:800; Wako, 019-19741). Confocal imaging and

743   cell quantification were performed. Confocal z-stack images were acquired on a Nikon A1

744   confocal laser microscope system (Japan). NIH ImageJ software was used to count cell numbers,

745   analyze mean fluorescence intensity of immunoreactive cells, and quantify Iba1 morphology

746   according to previous protocols [4]. Cell counts were performed in nine randomly selected sections

747   in each group.

748

749   **Activity and sleep pattern measurement**

750   Actical physical activity monitors (Respironics, Pennsylvania, USA) were used to monitor activity

751   levels of freely moving monkeys during the day (07:00 am–19:00 pm) and sleep patterns during

752   the night (19:00 pm–07:00 am). The monitors are water resistant (IEC Standard 60529 IPX7),

753   lightweight (16 g), and small in size ($2.9 \times 3.7 \times 1.1$ cm^3). The device was calibrated with monkey

754   information using Actical software before being placed on the monkey's neck by a soft belt. The

755   monitor was mounted on the same location on each subject to ensure consistency of the data. The

756   monitor uses a single internal omnidirectional accelerometer to sense motion in all directions and

757   integrates the amplitude and frequency of detected motion. The activity data were collected at a

758   sampling rate of 32 HZ and in epochs as short as 1 s. Each monkey was monitored for a period of

759   7–9 d (according to battery life).

760

761   The 7 d of activity was analyzed off-line, and sleep patterns were categorized in 1-min epochs

762   using the night-time data into three states, i.e., awake, transitional, and relaxed sleep [5]. According

763   to previous literature, the animal was considered awake when locomotion occurred or when three

764   or more movements occurred within 1 min. Sleep was scored as transitional when one or two

765   movements occurred within 1 min. The relaxed sleep state was assigned when the animals

766   exhibited no body or limb movements. Sleep duration was the sum of all 1-min epochs of different

767 states (transitional or relaxed sleep) and sleep fragmentation was defined as the frequency of

768 waking bouts lasting 1 min or longer per night.

769

770 **Social interaction test**

771 Social interaction tests were conducted, in which behaviors were video-recorded in social

772 groupings (6–8 male monkeys of similar age) and analyzed off-line to assess social interaction

773 changes among different manipulations [5]. In this study, measured behaviors included active

774 social contact, aggressive, submissive, and stereotypical behaviors. Active social contact was

775 defined as initiating social contact, such as playing, grooming, sharing toys, and sitting together

776 (within another monkey's reach or in contact) between two and/or more monkeys [6]. Aggressive

777 behaviors included biting, grabbing, slapping, open-mouth threats, stare-threats, chasing, and

778 forced displacement. Submissive behavior was defined as screaming, crouching, fleeing, lip

779 smacking, submissive presenting, grimacing, or escaping[7, 8]. Stereotypical behavior was defined

780 as repetitive and consistent actions with no apparent purpose, including digit (finger or toe) sucking,

781 pacing (repetitive, ritualized movement usually involving circling the cage), self-grasping

782 (grabbing or holding onto part of their own body), bouncing (jumping up and down on all four

783 legs), rocking (back and forth movement of the upper body with still feet), body spasms (a quick

784 shake of the body), cage shaking (any vigorous shaking of the cage), and lip-smacking (pursing

785 the lips together and moving them to produce a smacking sound) [9]. Each monkey's behavior was

786 video-recorded at the same time in the morning (09:30 am–11:30 am) or in the afternoon (14:00

787 pm–16:00 pm) for 7 d (avoiding rainy days). The behaviors were scored as frequencies and

788 durations per hour by three double-blind viewers. The behaviors were marked when the monkey

789 was unobscured and the viewers could clearly observe behaviors.

790

791 **Social reward test**

792 Social reward was studied using the social conditioned place preference (CPP) test, as employed

793 in previous studies [10]. The apparatus for the social CPP test was divided into two equally sized

794 acrylic cages ($100 \times 100 \times 100$ cm), with an opening (25×40 cm) at the base. The two cages were

795 different colors (white versus red) and could be easily discriminated by the monkey. After 5 d of

796 adaptation to the test chamber (30 min per day per monkey), the formal experiment was

797 commenced. We initiated 30 min of video analysis per day (pre-conditioning trial) to establish

798 color preference (baseline) for the two chambers (white or red). After 3 d of testing, all six

799 monkeys exhibited preference for the red chamber. The monkeys then underwent isolation

800 conditioning for 24 h in the preferred (red) cage, followed by 24 h of social conditioning (with one

801 female cage-mate) three times in the non-preferred (white) cage. After this, each monkey

802 underwent a 30-min postconditioning trial to measure its preference for the two cages. The amount

803 of time spent freely exploring each cage during the 30-min postconditioning trial was recorded.

804 The–duration time (time spent) in the social cage was compared between the pre- and post-

805 conditioning trials to demonstrate whether the monkey established preference for the social

806 conditioning cage (Fig. S5).

807

808 **Active avoidance test**

809 A modified version of the active avoidance apparatus was used to evaluate fear responses of the

810 monkeys to loud noise. The equipment included two plexiglass observation chambers (80 × 80 ×

811 80 cm) connected by a tunnel (60 × 40 × 20 cm). In each chamber, one remote-controlled high-

812 pitch loudspeaker (116 dB) was installed. A video camera was used to record monkey behavior.

813 Each monkey was tested once daily at the same time for 3 d. Before the test, each monkey was

814 trained to follow a monkey guide stick to enter the test chamber and adapt to free shuttling between

815 the two chambers over several days. Afterwards, the monkey was guided with the stick from the

816 home cage into the test chamber. Each monkey was given 10 min to adapt to the chamber, after

817 which a loud noise (116 dB) was presented, which should elicit an escape response from the

818 monkey to move to the adjoining chamber. The noise was stopped when the monkey escaped to

819 the other chamber. To ensure no harm was inflicted, the noise was stopped after 2 min if the

820 monkey had not successfully escaped. Escape time from the noise chamber to the quiet chamber

821 was recorded [5].

822

823 **Gaze-following test**

824 A monkey's ability to follow another's gaze can be assessed using a gaze-following test. Unlike

825 adults, juveniles are not able to orient their attention on the basis of another's gaze alone[11].

826 Therefore, head-eye cues were presented to the monkeys to determine differences in gaze-

827 following ability between the Cas9-MECP2 and Cas9-Control monkeys. During the test, the

828 experimenter sat facing the monkey at a 1.5-m distance, and then turned his/her head 70° up, down,

829   left, or right and maintained each posture for 3 s, with the eyes always aligned with the head. In

830   the test, for each head orientation, a total of 25 trials were carried out randomly (100 trials per day).

831   Each monkey was tested under freely moving conditions at the same time of the day. The responses

832   of the monkeys were recorded by a video camera positioned behind the experimenter. A trial was

833   considered valid only if the monkey was looking at the experimenter at the beginning of the trial.

834   Each monkey was tested for three consecutive days and the percentage of gaze-following

835   responses (number of responses divided by total number of valid trials in each test session) was

836   calculated. To control for the possible effect of differences in attention to the experimenter between

837   the Cas9-MECP2 and Cas9-Control monkeys, 5 min of behavioral analysis was scored randomly

838   during each test session. The amount of time in which the monkey's body was oriented toward the

839   experimenter and the monkey visually explored the experimenter was totaled [11] (Fig. S6).

840

Modified Brinkman board test

842   This test, modified and adapted from previous reports, is widely used for assessing manual

843   dexterity in non-human primates [12]. Behavioral assessment of manual dexterity is based on

844   manual grasping tasks (use of precision grip to obtain peanut kernel). Briefly, monkeys retrieve a

845   peanut kernel from 21 slots of different size (four 1×2 cm, four 1.5×2 cm, four 2×2 cm, three

846   1×3 cm, three 1.5×3 cm, and three 2×3 cm). Two parameters (accuracy and contact time) were

847   analyzed by replaying the recorded video sequences. Accuracy: correct rate of retrievals of peanut

848   kernel from slots. Contact time: time interval between first finger touch of the pellet and onset of

849   retrieval of the pellet from the well. Time interval was measured by replaying the video sequence

850   frame-by-frame.

851

Gait speed

853   Gait speed is a reflection of motor processes[13]. To observe whether the Cas9-MECP2 monkeys

854   exhibited motor disabilities, we measured gait speed following previous study [13]. Briefly, usual

855   walking speed was quantified by offline video analysis from 5 d of interference-free video

856   surveillance recording (09:30 am–16:30 pm). Only monkeys traversing a minimum of 1 m at a

857   normal pace without any motivation, such as food or provocation, were analyzed. Five valid

858   instances per monkey were used for statistical analysis.

859

Reversal learning (RL)

Reversal learning tasks are used to assess learning ability and cognitive flexibility[14]. Here, testing was conducted in a Wisconsin General Test Apparatus (WGTA). Monkeys were familiar with the WGTA and fasted before the experiment. First, monkeys were taught to flip the cover and obtain peanuts from the food well. Second, two different shaped covers ("◇" and "☆") were used to cover two food wells, with the peanut always placed in the food well covered by "☆". The "☆" was placed (right or left) randomly, and monkeys could only select one of the two shapes ("◇" or "☆"). Only when the monkey selected "☆" was it able to obtain the peanut. When the monkey's peanut success rate was above 85% in 45 successive trails, we added two new shapes ("○" and "♡"), with the peanut always placed in the food well covered by "♡". The four shapes appeared randomly with equal probability in a session (16 trials). When the monkey's peanut success rate was above 85% in three successive sessions, we started the reverse task, where selecting "○" and "◇" achieved peanuts. The number of trials required until the monkey reached an 85% success rate in a session was recorded.

Pattern-recognition task

A modified version of the pattern-recognition task was used to evaluate memory ability [15]. Testing was conducted in a WGTA. Monkeys were familiar with the WGTA and fasted before the experiment. Five different shaped covers were used to cover five food wells. The position of the cover was randomly decided by the computer, with peanuts only found under one shaped cover. The monkeys first learned two shapes and gradually increased to learning all five shapes. When a monkey's peanut success rate was above 90% in 60 successive trails, it was considered to have remembered the reward graphic. After one week, the monkey performed the task again, and the correct choice rate of the reward graphic was counted.

***In vivo* mutation efficiency detection**

To detect whether gene editing occurred in the monkey brain tissue near the injection sites, fluorescent-positive tissue was collected from slices and then digested by protease K. Genome DNA was extracted by phenol-chloroform and precipitated by absolute alcohol. The proximal

889   regions of the sgRNA-targeting sites were amplified by PCR, followed by Sanger sequencing.

890   Results were compared with wild-type control to confirm whether the target gene was edited.

891

892   **Off-target detection**

893   To detect the possible presence of sgRNA off-targeting, an online database

894   (http://www.rgenome.net/cas-offinder/) was used to predict potential off-target sites. From the

895   many potential off-target sites, several of the most likely sites were selected (Table S3). These

896   selected sites had to satisfy the following conditions: must be located in the *Macaca mulatta*

897   Mmul_10 reference genome database; the five bases on the sgRNA next to PAM (seed region)

898   must be free from mismatch; total number of mismatched bases must be less than or equal to three;

899   and, bulge size must be less than or equal to one. The proximal regions of these selected potential

900   off-target sites were amplified by PCR, followed by Sanger sequencing. Results were compared

901   with wild-type control to confirm whether real off-target sites existed.

902

903

904

905

906

Supplementary Figures:
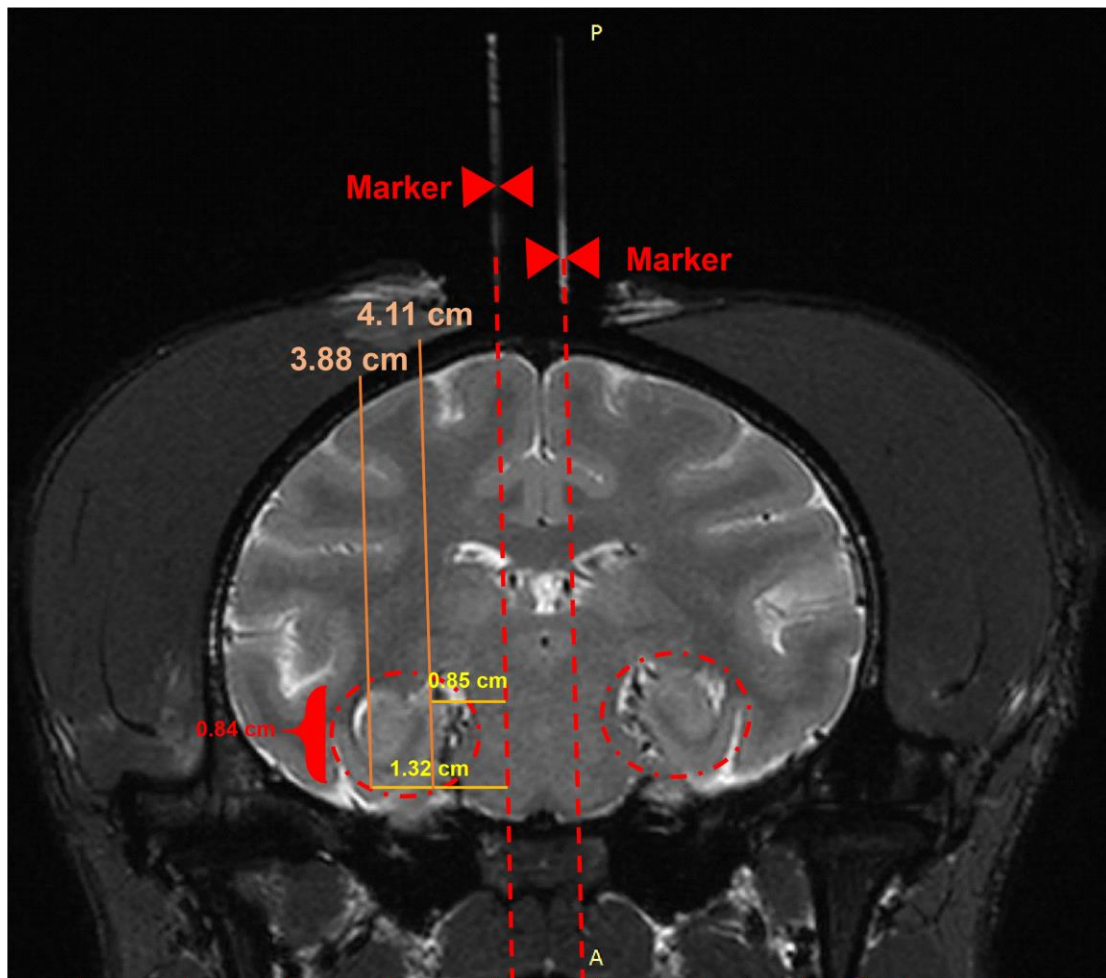
Figure S1. MRI images of marker locations, hippocampus, and coordinates of injection pathways. MRI image displays monkey-skull markers (red arrows), which were used as references to locate hippocampus in coronal plane. Red circles indicate location of hippocampus and red number shows range of injection depths). Orange and yellow numbers show maxima and minima coordinates of injection pathways in this section, respectively.

915

916

Figure S2. Identification of genetic mutations caused by SaCas9 and sgRNAs. Examples of monoclone mutations near target site caused by sgRNA in Cas9-MECP2 (KO-3) and Cas9-Control monkey (Ctrl-2) brains. Red highlights show mutated base and amino acid, and blue highlights show sgRNA target sites.
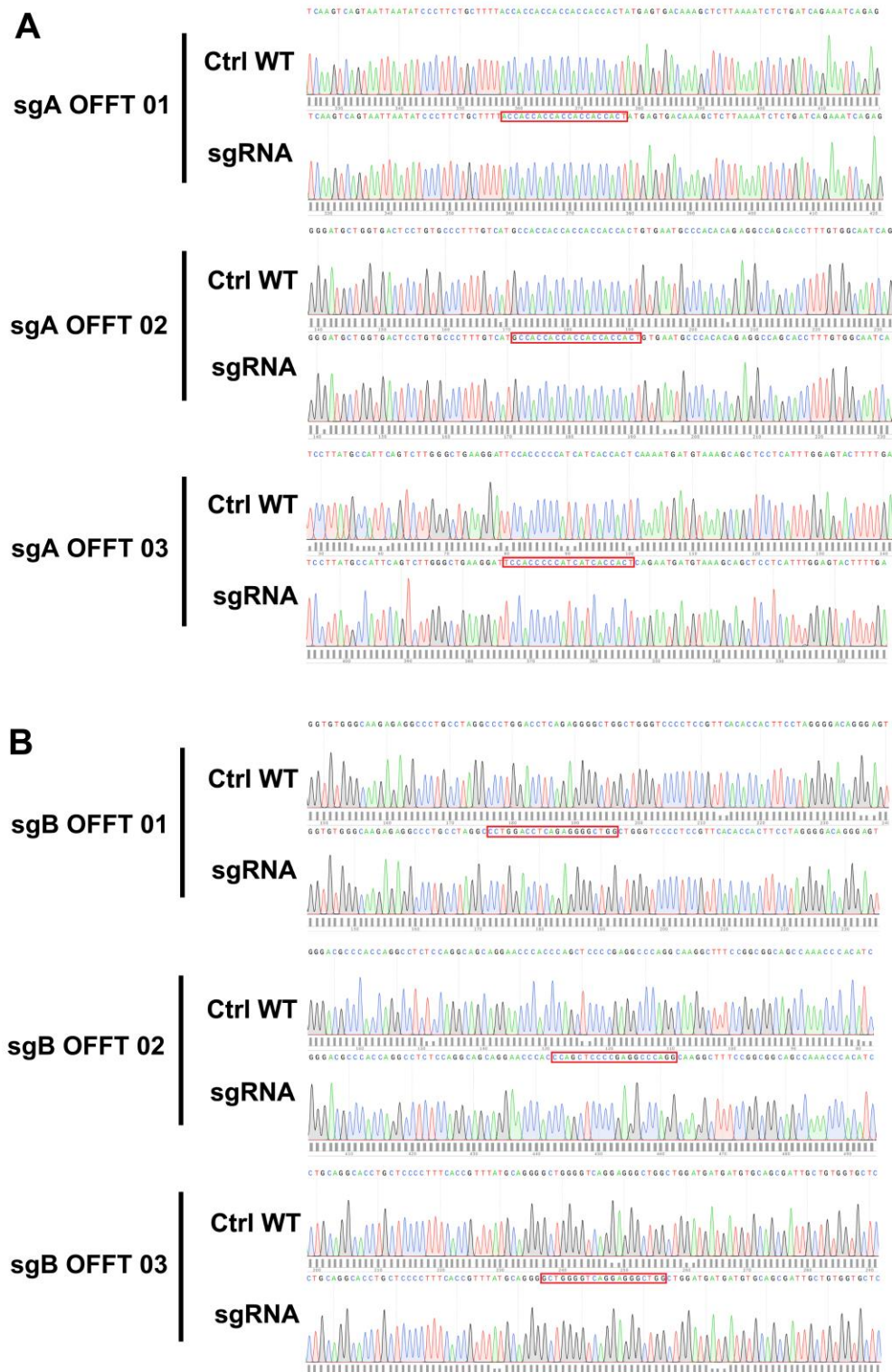
920

921

922

923

924

925

926

Figure S3. Sequencing results of predicted off-target sites. Potential off-target sites of sgRNA1 (A) and sgRNA2 (B) were predicted using Cas-OFFinder database (http://www.rgenome.net/cas-offinder/). Typical sequencing results are shown and compared with genome sequences of wild-type monkeys.
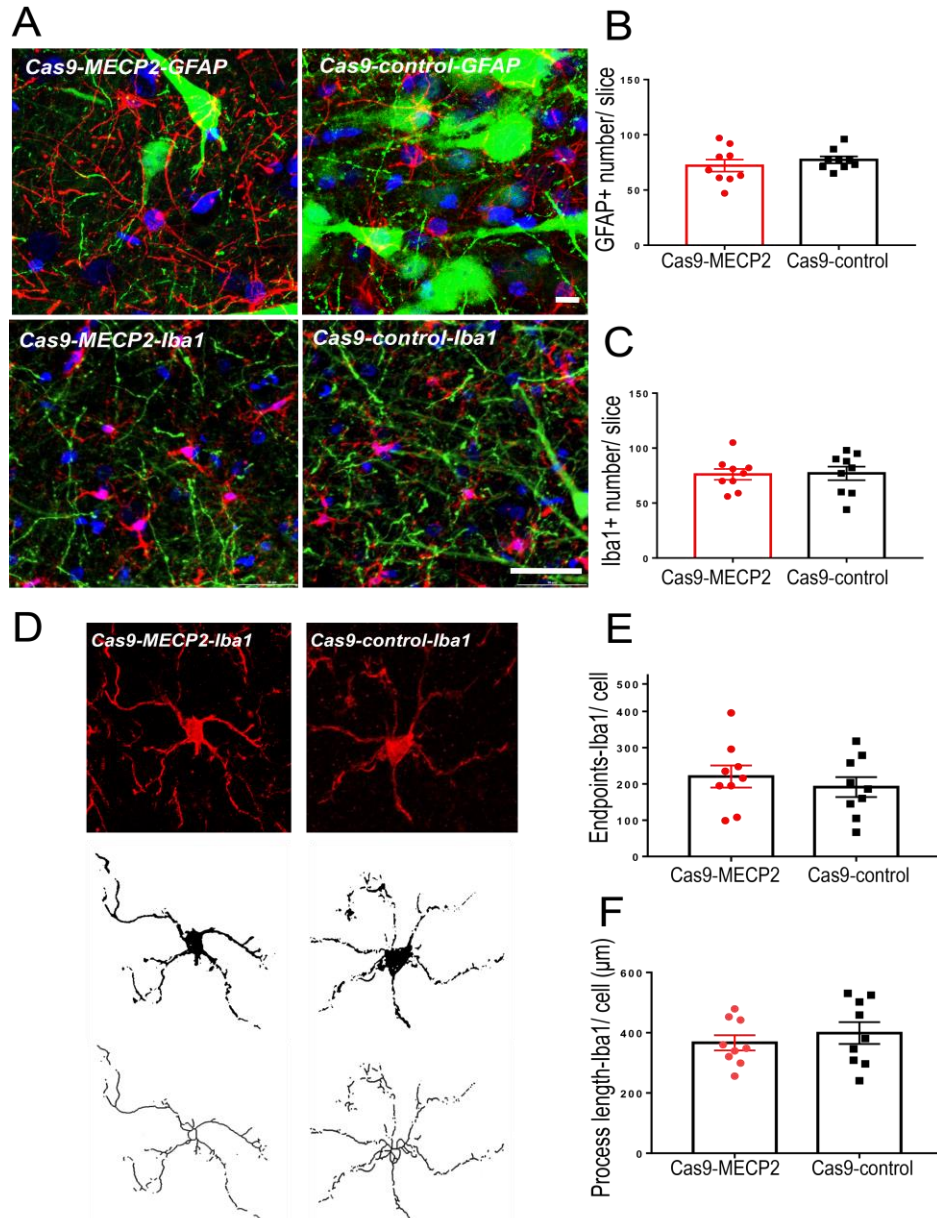
930

931
932 **Figure S4. Immunohistochemical analysis of astrocytes and microglial cells.**
933 (A) GFAP-positive astrocytes and Iba1-positive microglial cells in AAV-transduced brain area (GFP (green), GFAP
934 (red), Iba1(red), and DAPI (blue); GFAP bar = 10 µm; Iba1 bar = 50 µm). (B) No significant differences were found
935 in number of GFAP-positive astrocytes between Cas9-MECP2 (n = 9 slices) and Cas9-Control groups (n = 9 slices,
936 Mann Whitney test, $p = 0.4755$). (C) No significant differences were found in number of Iba1-positive microglial cells
937 between Cas9-MECP2 (n = 9 slices) and Cas9-Control groups (n = 9 slices, Mann Whitney test, $p = 0.6196$) (D)
938 Example photomicrograph of fluorescent IHC and cropped cell with skeletonized image. There were no significant
939 differences in (E) endpoints (Mann Whitney test, $p = 0.5302$) or (F) process lengths (Mann Whitney test, $p = 0.5457$)
940 in Iba1 cells between Cas9-MECP2 (n = 9) and Cas9-Control groups (n = 9). Data are means ± SEM.
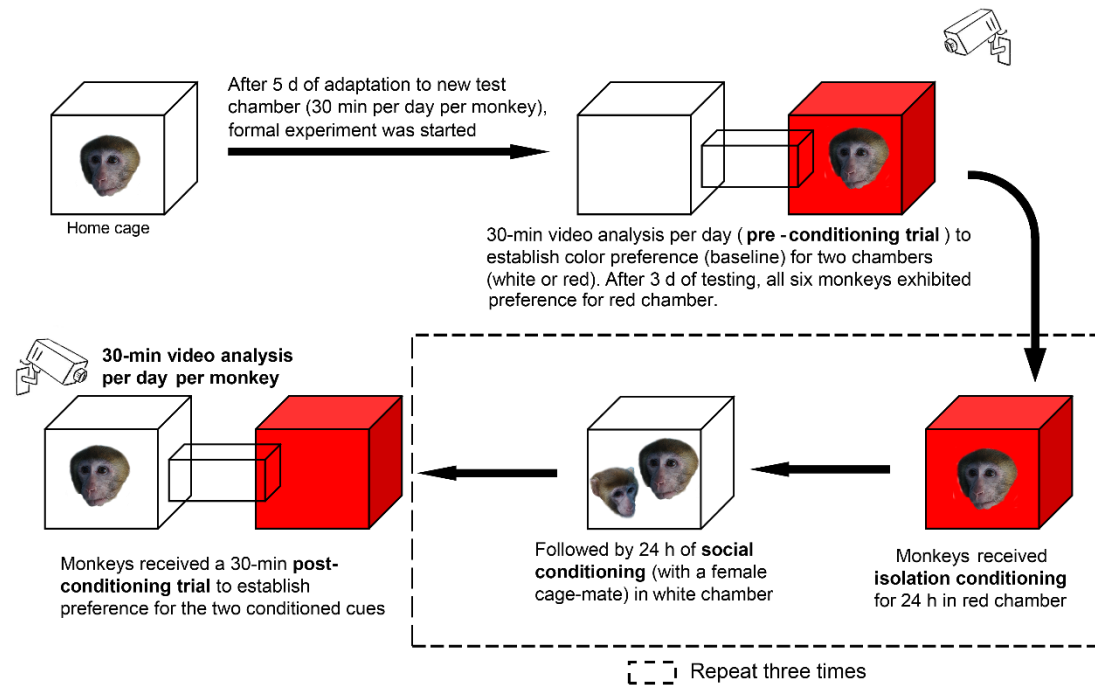**941**

942

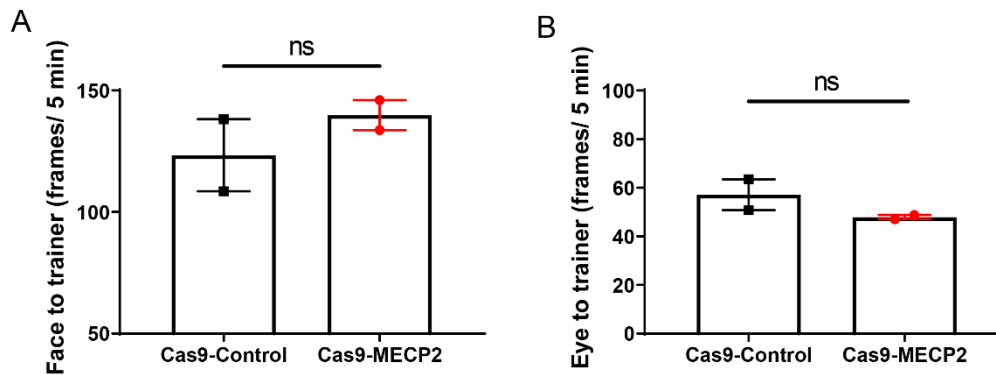**Figure S5. Schematic of social reward test procedure**

944

945

946

947 **Figure S6. Controls for GFR test**
948 There were no significant differences between Cas9-MECP2 and Cas9-Ctrl monkeys in: (A) amount of time in which
949 monkey's body was oriented toward experimenter (Mann Whitney test, $p = 0.6667$) and (B) monkey looked at
950 experimenter (Mann Whitney test, $p = 0.33$). Data are means $\pm$ SEM.
951
952

953
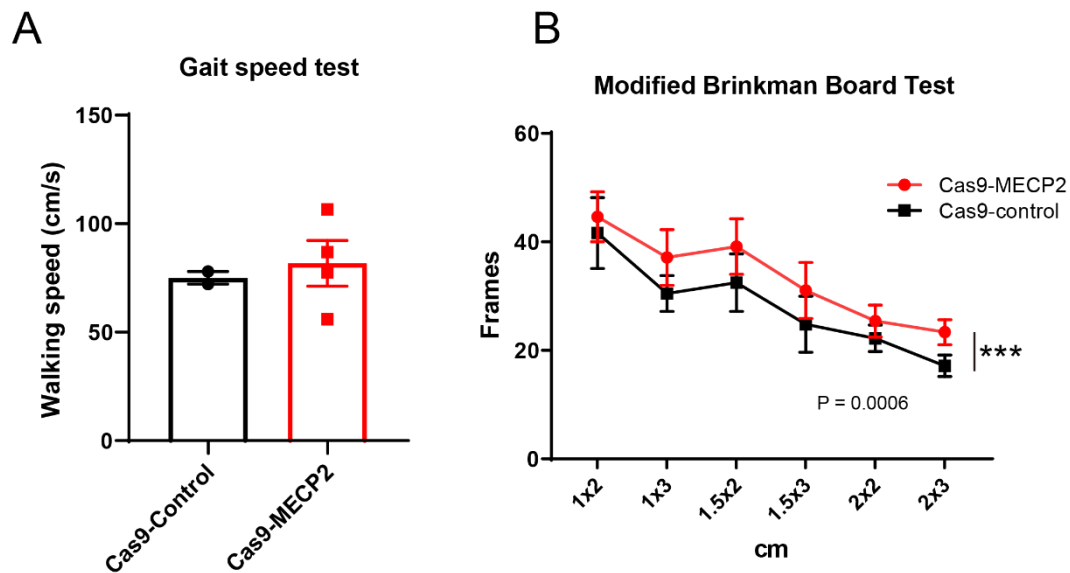
954 **Figure S7.** (A) Walking speed (cm/s) of Cas9-MECP2 (n = 4) and Cas9-Control groups (n = 2). Average of five
955 samples over 5 d of walking speed test is depicted (Mann Whitney test, p = 0.3675), data are means ± SEM. (B)
956 Modified Brinkman board test was used to assess manual dexterity. There was significant difference in latency to grab
957 peanut kernel from grid between Cas9-MECP2 (n = 5) and Cas9-Control groups (n = 3, p = 0.0006). Average of 21
958 samples per monkey over three consecutive days is depicted, data are means ± SEM..
959
960

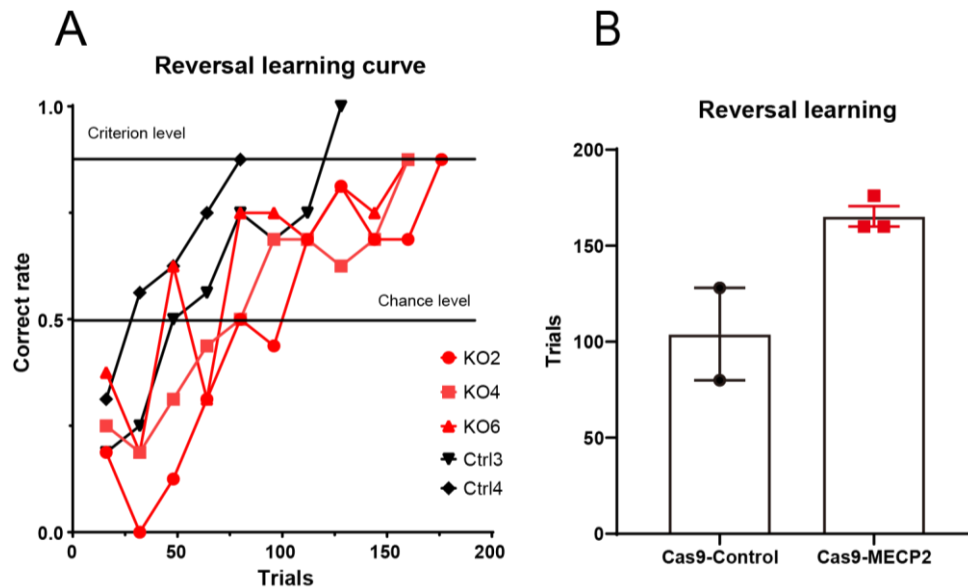**Figure S8. Performance of reversal learning task of two groups of monkeys** (A) Learning curve with reverse task in Cas9-MECP2 (n = 3) and Cas9-Control monkeys (n = 2), and (B) number of final trials to reach criterion level showed no significant differences between Cas9-MECP2 and Cas9-Control groups ($p = 0.1$). Data are means ± SEM. Non-parametric tests (Mann Whitney) were used for statistical analysis.

Figure S9. Performance of pattern recognition and memory retrieval tasks of monkeys with gene editing. During learning phase, (A) learning curve and (B) number of final trials to reach criterion level showed no significant differences between Cas9-MECP2 ($p = 0.3$, n = 3) and Cas9-Control groups (n = 2). During memory retrieval phase, (C) there was no significant difference in correct rate between groups ($p = 0.4$). Data are means ± SEM. Non-parametric tests (Mann Whitney) were used for statistical analysis.

975

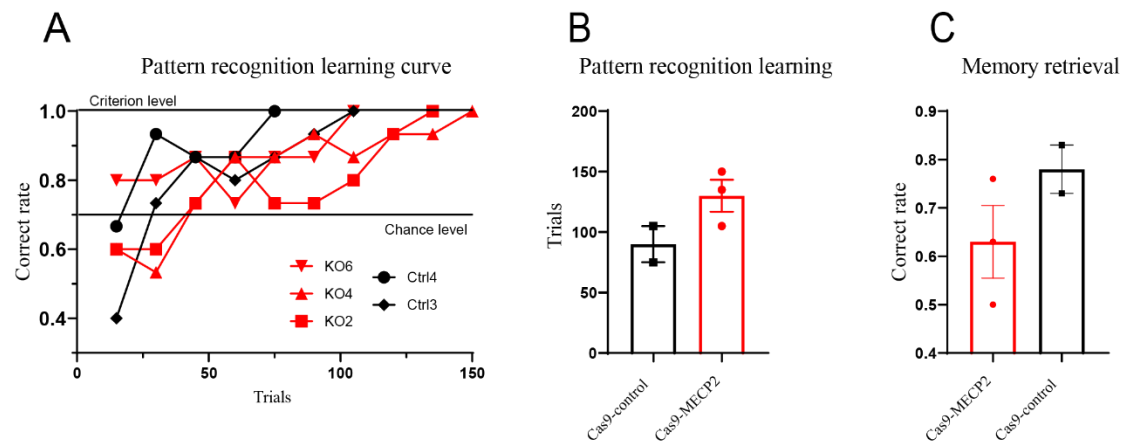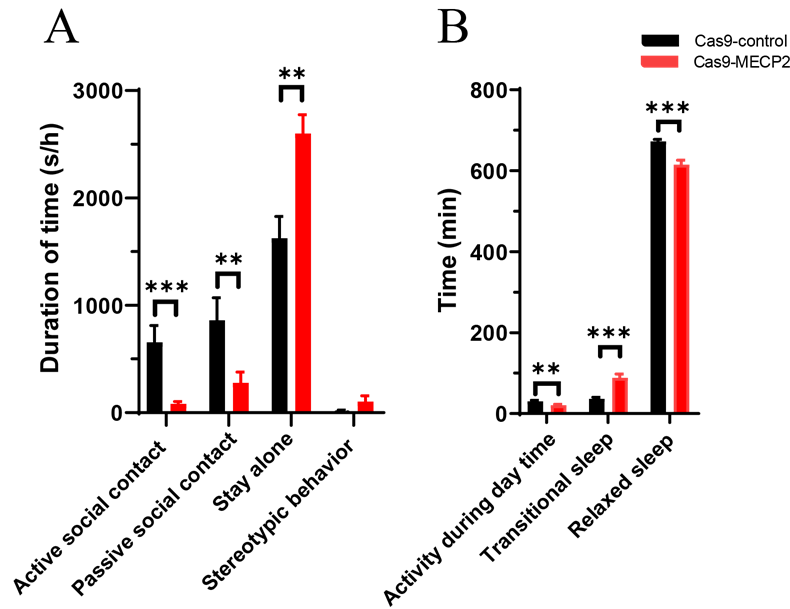**Figure S10. longitudinal analysis of social behaviors, light/dark activities, and sleep patterns consistently showed ASD phenotypes.** (A) Duration of active social contact ($p = 0.0002$), passive social contact ($p = 0.0047$), stay alone ($p = 0.0038$), and stereotypic behavior ($p = 0.143$) of Cas9-MECP2 and Cas9-Control monkeys. (B) Compared to Cas9-contorl monkeys, Cas9-MECP2 monkeys showed decreased day-time activities ($p = 0.0028$), longer transitional sleep time ($p < 0.0001$), and shorter relaxed sleep times ($p < 0.0001$). Data were averaged over 5 d and showed means ± SEM, $* p < 0.05$, $** p < 0.01$, $*** p < 0.001$. Non-parametric test (Mann Whitney) was used for statistical analysis.

983
984

985   **Table S1.** Information on individual monkeys for behavioral tests.

Table S1A. Social interaction and stereotypic behavior

ID	Age at gene editing (years old)	Days after gene editing
Ctrl-1	3	93
Ctrl-2	3	91
Ctrl-3	2	109
KO-1	3	157
KO-2	2	154
KO-3	3	97
KO-4	3	95
KO-5	3	93
KO-6	3	92
KO-7	3	91

986

Table S1B. Light activity and sleep patterns

ID	Age at gene editing (years old)	Days after gene editing
Ctrl-1	3	93
Ctrl-2	3	91
Ctrl-3	2	109
KO-3	3	98
KO-4	3	95
KO-5	3	93
KO-6	3	92

987

Table S1C. Social reward test

ID	Age at gene editing (years old)	Days after gene editing
Ctrl-2	3	507
Ctrl-3	2	256
Ctrl-4	2	247
KO-4	3	633
KO-6	3	198
KO-7	3	190

988

Table S1D. Gaze following test

ID	Age at gene editing (years old)	Days after gene editing
Ctrl-3	2	95
Ctrl-4	2	91
KO-6	3	101
KO-7	3	97

989

Table S1E. Active avoidance test

ID	Age at gene editing (years old)	Days after gene editing
Ctrl-3	2	138
Ctrl-4	2	139
KO-6	3	108
KO-7	3	105

990

Table S1F. Gait speed test

ID	Age at gene editing (years old)	Days after gene editing
Ctrl 3	2	680
Ctrl 4	2	679
KO 2	2	1414
KO4	3	1048
KO 6	3	614
KO 7	3	613

991

992

Table S1G. Brinkman board test

ID	Age at gene editing (years old)	Days after gene editing
Ctrl-2	3	384
Ctrl-3	2	124
Ctrl-4	2	125
KO 2	2	753
KO4	3	416
KO 5	3	298
KO 6	3	121
KO 7	3	125

993

Table S1H. Reversal learning

ID	Age at gene editing (years old)	Days after gene editing
Ctrl 3	2	708
Ctrl 4	2	707
KO 2	2	1442
KO4	3	1076
KO 6	3	642

994

Table S1I. Pattern recognition learning

ID	Age at gene editing (years old)	Days after gene editing
Ctrl 3	2	700
Ctrl 4	2	699
KO 2	2	1434
KO4	3	1068
KO 6	3	634

995

996

997

998 **Table S2.** Median value of injection coordinates of each monkey determined from MRI scans.

Monkey	Coordinates: Median of anterior-posterior/medial-lateral/deep/angle	Total injected vector volume (μL) for bilateral hippocampus
KO1	-1.3, -1, -0.9, -0, +0.3 +1 cm / ±12.5, ±16 cm /-2.9 ~ -3.8 cm / 0°	368
KO2	-1, -0.7, -0.4, -0.1, +0.2 cm / ±1.36 cm, ±1.80 cm /-2.75 ~ -3.61 cm / 0°	446
KO3	-0.7, -0.5, -0.3, -0.15 and +0.1 cm/ ± 1.25, ± 16 cm /-2.9~ -3.7 cm /0°	386
KO4	-1, -0.8, -0.6, -0.4, -0.2 / ±1.30, ±1.63 cm /-3.2 ~ -3.8 cm /0°	392
KO5	-1.5, -1.3, -1.1, -0.9, -0.7m/ ±1.31, ±1.58 cm /-2.70~-3.49 cm /0°	372
KO6	-1.6, -1.2, -0.8, -0.5 cm/ ±1.20, ±1.73 cm /- 3.24~ -3.99 cm / 0°	398
KO7	-0.9, -0.7, -0.5, -0.3, -0.1 cm/ ±1.08, ±1.64 cm / -3.31~ - 4.30 cm / 0°	388
Ctrl	-2.3, -1.9, -1.6, -1.3 cm/ ±1.1, ±1.5 /-3.2~ -4.1 cm /0°	402
Ctr2	-0.9, -0.6, -0.3, 0, +2 cm/ ±1.27, ±1.69 /-2.82~ -3.54 cm /0°	374
Ctr3	-1.2, -0.9, -0.6, -0.3 cm/ ±1.35, ±1.65 cm / -3.31~ -3.82 cm / 0°	400
Ctr4	-0.8, -0.6, -0.4, -0.2, 0 cm/ ±1.13, ±1.49 cm / -2.93~ -3.51 cm / 0°	388

999
1000 Note: Locations depict: distance before (-) or after (+) interaural (cm); distance left (+) or right (-) to midsagittal plane (cm); distance under (-) skull (mm); and angle from vertical line (°).

1001

1002

1003

1004 **Table S3.** Potential off-target sites predicted by Cas-OFFinder database.

Name	Primer sequence
mecp2 sg DP32 fo	GAGTCTTCTATCCGATCTGTG
mecp2 sg DP32 re	CTGGGCATCTTCTCCTCTT
sgA OFFT 01 DP fo	GAGGTATCTTCCATAACTTCAG
sgA OFFT 01 DP re	GTTGATGATGAGTGGCAATT
sgA OFFT 02 DP fo	ACTAAGGTGTTCTCAGACTG
sgA OFFT 02 DP re	ATTGCTGCTGGTGTGATT
sgA OFFT 03 DP fo	CCTTATGCCATTCAGTCTTG
sgA OFFT 03 DP re	CTTGGTGTCCACAGTTACTA
sgB OFFT 01 DP fo	GGCGTGGAGTAGATAAGTC
sgB OFFT 01 DP re	AGGATGGAGCCAGAGAAG
sgB OFFT 02 DP fo	CTCACCGAGGAACGATTG
sgB OFFT 02 DP re	CTGACTGAGCAAGTGTAGG
sgB OFFT 03 DP fo	GATGTCAGCGTAACTCAATG
sgB OFFT 03 DP re	CCTGCTTCCAACTCCTAAG

1005

1006

1007

Table S4. Ages of monkeys during social interaction, light activity, and sleep pattern during revision

ID	Age at surgery (years old)	Days after gene-editing surgery
Ctrl 3	2	680
Ctrl 4	2	679
KO 2	2	1414
KO4	3	1048
KO 6	3	614
KO 7	3	613

1008

1009

1010 **Movie details:**

1011 **Movie S1-3. Representative social behaviors changes of gene-edited monkey before and after**

1012 **gene-editing:** macaque showed close social interactions (grooming) with other macaques before

1013 virus injection (movie S1). After virus injection, the same macaque spent more time alone in corner

1014 (movie S2) and ignored social interactions initiated by other macaques (movie S3)

1015

1016 **Movie S4-5. Representative social reward behaviors:** after social conditioning, control macaque

1017 was more willing to stay in white social cage than previously preferred red cage (movie S4), while

1018 gene-edited macaque was still willing to stay in previously preferred red cage (movie S5).

1019

1020 **Movie S6-7. Representative gaze-following responses:** control monkey followed direction of

1021 experimenter's gaze (movie S6), while gene-edited monkey did not follow direction of

1022 experimenter's gaze (movie S7).

1023

1024 **Movie S8-9. Representative active avoidance responses:** when alarm sounded, control macaque

1025 quickly escaped to another cage (movie S8), while gene-edited macaque showed insensitivity to

1026 noise, and took a long time to escape to another cage (movie S9).

1027

1028

Supplemental References

1. Janet C. Garber, R.W.b., Joseph T. bielitzki, Leigh Ann Clayton, *Guide for the care and use of laboratory animals.* 2011: THE NATIONSL ACADEMIES.

2. Jing, W., et al., *A new MRI approach for accurately implanting microelectrodes into deep brain structures of the rhesus monkey (Macaca mulatta).* Journal of neuroscience methods, 2010. **193**(2): p. 203-209.

3. Wu, S.-H., et al., *Comparative study of the transfection efficiency of commonly used viral vectors in rhesus monkey (Macaca mulatta) brains.* Zoological research, 2017. **38**(2): p. 88.

4. Au - Young, K. and H. Au - Morrison, *Quantifying Microglia Morphology from Photomicrographs of Immunohistochemistry Prepared Tissue Using ImageJ.* JoVE, 2018(136): p. e57648.

5. Chen, Y., et al., *Modeling Rett syndrome using TALEN-edited MECP2 mutant cynomolgus monkeys.* Cell, 2017. **169**(5): p. 945-955. e10.

6. Qin, D., et al., *The first observation of seasonal affective disorder symptoms in Rhesus macaque.* Behavioural Brain Research, 2015. **292**(2015): p. 463-469.

7. Qin, D.D., et al., *Prolonged secretion of cortisol as a possible mechanism underlying stress and depressive behaviour.* Scientific Reports, 2016. **6**(30187).

8. Qin, D.D., et al., *Social rank and cortisol among female rhesus macaques (Macaca mulatta).* Zoological Research, 2013. **34**(2): p. E42.

9. Altmann, J., *Observational study of behavior: sampling methods.* Behaviour, 1974. **49**(3): p. 227-67.

10. Dölen, G., et al., *Social reward requires coordinated activity of nucleus accumbens oxytocin and serotonin.* Nature, 2013. **501**(7466): p. 179.

11. Ferrari, P.F., et al., *The ability to follow eye gaze and its emergence during development in macaque monkeys.* Proc Natl Acad Sci U S A, 2000. **97**(25): p. 13997-4002.

12. Schmidlin, E., et al., *Behavioral assessment of manual dexterity in non-human primates.* Journal of visualized experiments: JoVE, 2011(57).

13. Shively, C.A., et al., *Aging and physical mobility in group-housed Old World monkeys.* **34**(5): p. 1123-1131.

14. Izquierdo, A., et al., *The neural basis of reversal learning: An updated perspective.* 2016. **345**: p. 12-26.

15. Mishkin, M. and T. Appenzeller, *The anatomy of memory.* 1987. **256**(6): p. 80-9.

1062
1063
1064